iScience

Article

The role of Tim-3+T cell subsets in the peripheral blood of patients with COVID-19 and diabetes

Graphical abstract

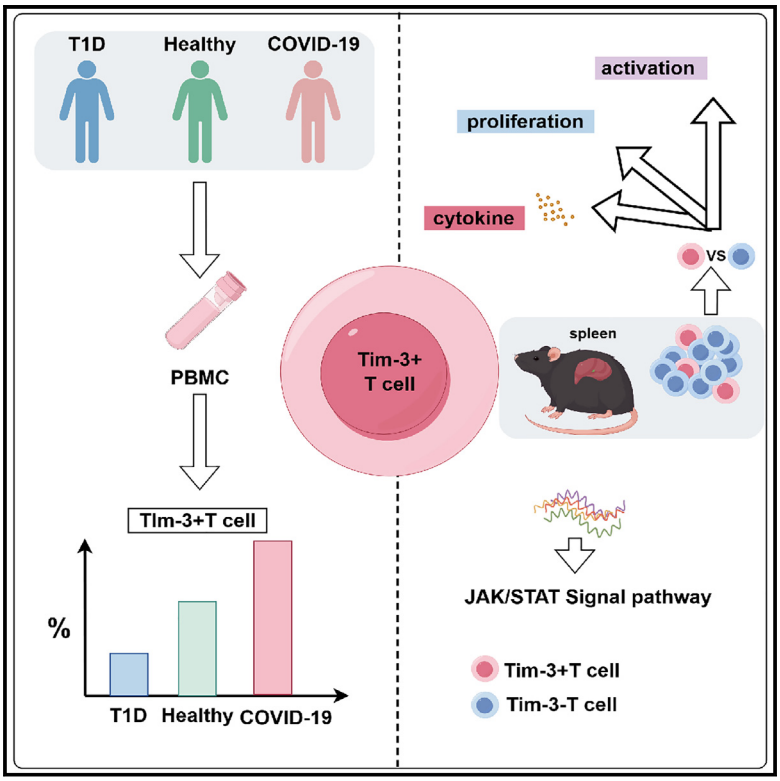

Highlights

- Altered Tim-3+ T cell subsets in patients with COVID-19 and T1D
- Tim-3+ T cells show impaired activation, proliferation, and cytokine secretion
- Downregulation of the JAK-STAT pathway in Tim-3+ T cells in disease conditions
- Tim-3+ T cells may play an important role in immunoregulation in COVID-19 and T1D

Authors

Wenjun Luo, Mingjiu Zhao, Mengyao Gu, Jiaqi Huang, Shiyao Wu, Bin Zhao

Correspondence

wushiyao@csu.edu.cn (S.W.), binzhao@csu.edu.cn (B.Z.)

In brief

Disease; Immune response; Immunology

Luo et al., 2025, iScience *28*, 112339
May 16, 2025
https://doi.org/10.1016/j.isci.2025.112339

CellPress

iScience

CellPress
OPEN ACCESS

Article

The role of Tim-3+T cell subsets in the peripheral blood of patients with COVID-19 and diabetes

Wenjun Luo,[1,4,5,6] Mingjiu Zhao,[1,4,5,6] Mengyao Gu,[1] Jiaqi Huang,[1,4,5] Shiyao Wu,[2,3,*] and Bin Zhao[1,4,5,7,*]

[1]National Clinical Research Center for Metabolic Diseases, Metabolic Syndrome Research Center, Key Laboratory of Diabetes Immunology, Ministry of Education, and Department of Metabolism and Endocrinology, The Second Xiangya Hospital of Central South University, Changsha, Hunan, China

[2]Department of Rheumatology and Immunology, Xiangya Hospital, Central South University, Changsha, Hunan, China

[3]Department of Dermatology and Immunology, National Clinical Research Center for Geriatric Disorders, Xiangya Hospital, Changsha, Hunan, China

[4]Furong Laboratory, Changsha, China

[5]CSU-Sinocare Research Center for Nutrition and Metabolic Health, Xiangya School of Public Health, Central South University, Changsha, Hunan, China

[6]These authors contributed equally

[7]Lead contact

*Correspondence: wushiyao@csu.edu.cn (S.W.), binzhao@csu.edu.cn (B.Z.)

https://doi.org/10.1016/j.isci.2025.112339

SUMMARY

Corona Virus Disease 2019 (COVID-19) and diabetes interact to influence disease severity, yet their combined immunological characteristics remain unclear. Here, we analyzed Tim-3+ T cells in patients with COVID-19, Type 1 Diabetes (T1D), or both conditions. COVID-19 reduced peripheral T cell subsets but increased Tim-3+ cells, while T1D and COVID-19 with T1D showed the opposite pattern. Patients with Type 2 Diabetes (T2D) exhibited no significant alterations. In human samples and mouse models, Tim-3+ T cells demonstrated impaired activation and cytokine production. RNA-seq analysis in mice and RT-PCR analysis in human samples together identified the dysregulation of the JAK-STAT pathway in Tim-3+ T cells. These findings highlight Tim-3-mediated JAK-STAT dysregulation in T-cells as a potential mechanism linking COVID-19 and T1D, offering insights for therapeutic targeting.

INTRODUCTION

Corona Virus Disease 2019 (COVID-19), caused by Severe Acute Respiratory Syndrome Coronavirus 2 (SARS-CoV-2), was rapidly spread worldwide and led to a significant global incidence and mortality rate.[1,2] Diabetes is a common chronic disease characterized by persistently high blood glucose levels. Prolonged and chronic hyperglycemia could lead to damage in multiple tissues and organs, as well as acute and chronic complications, impacting human health and increasing the burden on society's healthcare system, making it one of the important public health issues faced by China and the world.[3] Unlike the immune imbalance caused by exogenous antigens in COVID-19, T1D (Type 1 diabetes) is a chronic autoimmune disease characterized by the progressive destruction of pancreatic beta cells, while T2D (type 2 diabetes) is a chronic systemic metabolic disorder caused by a long-term combination of genetic and environmental factors.[4,5]

Despite the differing pathogenesis, diabetes is closely associated with COVID-19, as it is highly prevalent in patients with COVID-19 and is related to increased risks of severe COVID-19 and mortality.[6] Statistics show that during the first year of the COVID-19 pandemic, the incidence of T1D in children aged 0–14 in Romania increased significantly by 16.9%, from 11.4 per 100,000 in 2019 to 13.3 per 100,000 in 2020.[7] The incidence of T2D in the United States has significantly increased from the range of 10.6–14.6 per 100,000 population before the COVID-19 pandemic to 16.9 per 100,000 population in the first quarter of 2020.[8] The increased susceptibility to diabetes in patients with COVID-19 could be attributed to various complex and interconnected factors, including the accelerated occurrence of undiagnosed diabetes due to lifestyle changes, stress-induced hyperglycemia, damage to pancreatic beta cells caused by cytokine storms, and delayed recovery of beta cell damage due to the administration of steroids during hospitalization.[6–9] In contrast, the existence of diabetes might also promote the occurrence and development of COVID-19. A high glucose environment may alter the metabolic state of monocytes, potentially weakening their antiviral defense mechanisms.[10,11]

The adaptive immune system, including $CD4^+$ and CD8+T cells, plays a critical role in defending against pathogens and regulating self-immunity. Imbalance in T cell response is a key factor in the pathogenesis of diseases such as COVID-19 and type 1 diabetes. Immune checkpoints are a class of molecules that maintain self-immune tolerance and regulate the duration

and magnitude of peripheral tissue immune responses.[12–14] T cell immunoglobulin and mucin domain-containing protein 3 (Tim-3), encoded by the human gene *HAVCR2*, is a member of the Tim family and is involved in immune regulation.[15] Considered as an exhaustion marker for T cells, Tim-3 is primarily expressed in terminally differentiated CD4+T cells such as Th1 cells, Th17 cells, Treg cells, and CD8+T cells such as type 1 CD8+T cells (Tc1), as well as in other immune-related cells such as B cells, dendritic cells, mast cells.[16–20]

Tim-3 has been suggested to be involved in the pathogenesis of both COVID-19 and diabetes.[21–23] In COVID-19, Tim-3 is associated with disease severity, and changes in Tim-3+ T cells have also been observed in the peripheral blood of patients with T1D.[24,25] Research suggests that a high-glucose environment can directly promote SARS-CoV-2 replication and cytokine expression, making patients with uncontrolled blood glucose levels more susceptible to severe COVID-19.[10] In diabetic nephropathy, Tim-3 is considered a key regulatory factor in renal inflammation.[26] A retrospective study on COVID-19 treatment found that thymosin alpha 1 (Tα1) reduced Tim-3 expression on $CD8^+$ T cells in patients with COVID-19.[27]

Recent studies have identified Tim-3 as a marker of T cell exhaustion.[28] However, Tim-3+$CD8^+$ T cells with a distinct terminally exhausted phenotype, expressing granzyme, perforin, and IFN-γ, have also been observed in the bone marrow tumor microenvironment.[29] More recent research has highlighted increased Tim-3 expression on T cells in COVID-19, associating this increase with T cell exhaustion. Nevertheless, the regulatory mechanisms of Tim-3+ T cells in COVID-19 and diabetes still require further investigation.

In this study, we evaluated changes in peripheral blood lymphocyte subsets and Tim-3+ T cells in patients with COVID-19 and diabetes. We assessed the functional state of Tim-3+ T cells in both mouse models and healthy human PBMCs. Using RNA-seq, we observed the downregulation of the JAK/STAT pathway in mouse Tim-3+ T cells and identified reduced expression levels of JAK/STAT pathway-related genes in Tim-3+ T cells from patients with COVID-19 and T1D. Our study characterizes immunoregulatory mechanisms of Tim-3+ T cells in COVID-19 and diabetes, suggesting potential implications for disease diagnosis and treatment.

RESULTS

Demographic and clinical characteristics of different disease subgroups

The clinical information and laboratory data for the healthy control, patients with COVID-19 with different severities, patients with different types of diabetes (T1D and T2D), and patients with COVID-19 with different diabetes (COVID-19 with T1D and COVID-19 with T2D) were shown in Tables 1, 2, and 3. The median ages for each group were as follows: 48.4 years for healthy controls, 67.5 years for mild to moderate COVID-19 cases, 71.3 years for severe COVID-19 cases, 36.1 years for patients with T1D, and 58.5 years for patients with T2D. Among patients with COVID-19 with diabetes, the median age was 48.1 years for those with T1D and 66 years for those with T2D. In our analysis, we accounted for disease onset characteristics and used analysis of covariance (ANCOVA) to adjust for the impact of age. Table 1 shows the demographic and clinical data for the healthy control group and patients with COVID-19 (mild-to-moderate COVID-19 and severe COVID-19). The results indicate that alanine aminotransferase (ALT) and aspartate aminotransferase (AST) levels in patients with COVID-19 were significantly higher than those in the healthy control group. Additionally, the percentage of lymphocytes in patients with severe COVID-19 was significantly lower than in the healthy control group, while the percentage of neutrophils and D-dimer levels were significantly higher. Table 2 shows the demographic and clinical data for the healthy control group and patients with diabetes (T1D and T2D). The results indicate that both patients with T1D and T2D had significantly higher fasting blood glucose and glycated hemoglobin levels compared to the healthy control group. Additionally, the percentage of monocytes in patients with T1D was significantly higher than in patients with T2D, and the low-density lipoprotein cholesterol levels were significantly higher than those in the healthy control group. Table 3 shows the demographic and clinical data for patients with COVID-19 alone and those with COVID-19 combined with different types of diabetes (COVID-19 with T1D and COVID-19 with T2D). The low-density lipoprotein cholesterol levels in patients with COVID-19 and T1D were significantly higher than in those with COVID-19 and T2D. The fasting blood glucose levels in patients with COVID-19 and T2D were significantly higher than those in patients with COVID-19 alone. Both glycated hemoglobin levels in patients with COVID-19 and T1D and those with COVID-19 and T2D were significantly higher than in patients with COVID-19 alone. Additionally, the blood urea nitrogen levels in patients with COVID-19 and T2D were significantly higher than those in patients with COVID-19 alone.

IMMUNOLOGICAL CHARACTERISTICS OF DIFFERENT DISEASE SUBGROUPS

We investigated the changes in peripheral T and B lymphocyte subsets among healthy controls, patients with mild-to-moderate COVID-19, and patients with severe COVID-19 (Figure 1A). As shown in Figure 1, compared to the healthy control group, patients with COVID-19 exhibited a significant decrease in CD4+T cells and $CD8^+$ T cells, with this alteration being particularly pronounced in patients with severe COVID-19 (Figure 1B). There were no significant changes in memory T cells and naive T cells among patients with severe mild-to-moderate and severe COVID-19 (Figure S1A). In comparison to both the healthy control group and patients with severe COVID-19, patients with mild-to-moderate COVID-19 showed a significant decrease in CD19+B cells. Patients with COVID-19 exhibited a trend of increased antibody-secreting cells (ASCs), while memory B cells showed no significant changes (Figures S2A and S2C). The cell count statistics indicate that the T cell subset counts in patients with COVID-19 have significantly decreased compared to healthy controls (Figure S3).

We assessed the proportions of peripheral T lymphocyte subsets in patients with T1D, patients with T2D, and healthy controls (Figure 1A). The results indicated a significant increase in the frequencies of $CD4^+$ and CD8+T cells in patients with T1D compared to healthy controls and patients with T2D (Figure 1C). We further

Table 1. Characteristics of healthy control and patients with COVID-19 with different severities recruited into the study

Characteristics	Healthy control	Mild/Moderate COVID-19	Severe COVID-19	*p* value between groups
Number	36	24	18	
Age (year)	48.4 ± 18.9	67.5 ± 17.5	71.3 ± 7.8	
Male (n,%)	13(36.1%)	10(41.7%)	11(61.1%)	0.13
Leukocyte count ($\times10^9$/L)	7.2 ± 3.0	6.4 ± 2.0	8.6 ± 2.9	0.05
Hemoglobin (g/L)	120.5 ± 21.5	117.4 ± 20.34	122.6 ± 18.2	0.77
Erythrocyte count ($\times10^{12}$/L)	4.2 ± 0.6	3.9 ± 0.8	4.0 ± 0.6	0.51
Platelet count ($\times10^9$/L)	223.6 ± 62.2	250.4 ± 119.2	274.1 ± 77.4	0.25
Neutrophil count ($\times10^9$/L)	3.8 ± 3.2	2.0 ± 2.9	2.9 ± 3.7	0.19
Neutrophil percentage (%)	65.7 ± 8.7	70.7 ± 9.5	76.3 ± 15.4$^{\#}$	0.015*
Lymphocyte count ($\times10^9$/L)	1.7 ± 0.6	1.4 ± 0.6	1.3 ± 1.1	0.08
Lymphocyte percentage (%)	26.0 ± 7.7	20.4 ± 8.9	15.0 ± 13.6$^{\#\#}$	0.004**
Monocyte count ($\times10^9$/L)	0.4 ± 0.2	0.5 ± 0.3	0.7 ± 0.7	0.07
Monocyte percentage (%)	6.4 ± 2.0	7.5 ± 3.5	7.0 ± 3.8	0.52
PCT (ng/mL)	0.026 ± 0.016	0.2 ± 0.4	0.3 ± 0.4	0.50
CRP (mg/L)	1.4 ± 1.2	22.1 ± 31.4	37.8 ± 47.9	0.10
IL-6 (pg/mL)	3.3 ± 2.0	4.3 ± 3.3	18.4 ± 16.9	0.034*
D-dimer (μg/mL)	0.4 ± 0.2	0.8 ± 0.7	1.5 ± 1.4$^{\#\#}$	0.013*
TG (mmol/L)	1.3 ± 0.8	1.5 ± 1.0	1.7 ± 1.1	0.46
TC (mmol/L)	4.2 ± 1.0	4.1 ± 1.0	4.3 ± 0.5	0.70
HDL-C (mmol/L)	1.1 ± 0.4	1.1 ± 0.3	0.9 ± 0.2	0.28
LDL-C (mmol/L)	2.7 ± 0.9	2.5 ± 0.9	2.9 ± 0.5	0.41
ALT (U/L)	18.0 ± 10.3	31.7 ± 19.9$^{\#}$	37.0 ± 23.1$^{\#\#}$	0.005**
AST (U/L)	19.0 ± 7.2	30.0 ± 16.5$^{\#}$	35.0 ± 14.6$^{\#\#}$	<0.001***
TBIL (μmol/L)	8.5 ± 3.0	9.3 ± 4.0	9.5 ± 4.2	0.72
DBIL (μmol/L)	3.1 ± 1.2	3.7 ± 2.2	3.9 ± 2.1	0.35
CR (μmol/L)	63.7 ± 16.2	75.4 ± 31.9	83.9 ± 43.4	0.10
25-hydroxyl-VitaminD (nmol/L)	48.4 ± 16.4	47.1 ± 18.3	36.1 ± 9.5	0.18
HbA1c (%)	5.7 ± 0.6	6.0 ± 0.3	6.1 ± 0.6	0.33
FBG (mmol/L)	4.9 ± 1.1	5.1 ± 1.0	5.5 ± 0.8	0.49

Data are expressed as the mean ± standard deviation for qualitative data.
PCT, procalcitonin; ESR, erythrocyte sedimentation rate; CRP means C-reactive protein.
TG, triglyceride; TC, total cholesterol; HDL-C, high density lipid-cholesterol; LDL-C, low density lipid-cholesterol; ALT, alanine aminotransferase; AST, aspartate transaminase; TBIL, total bilirubin; DBIL, conjugated bilirubin; CR, creatinine; FBG, fasting blood glucose.
Differences between groups: $^{*}p < 0.05$, $^{**}p < 0.01$, $^{***}p < 0.001$.
In comparison with healthy control: $^{\#}p < 0.05$, $^{\#\#}p < 0.01$.

investigated the proportions of peripheral blood lymphocyte subsets in patients with pure COVID-19 and those with combined T1D or T2D (Figure 1A). The results showed that patients with COVID-19 combined with T1D had a higher frequency of CD4+T cell subsets than both pure patients with COVID-19 and patients with COVID-19 combined with T2D (Figure 1D). Additionally, patients with COVID-19 combined with T1D exhibited a higher frequency of CD8+T cell subsets compared to those with COVID-19 combined with T2D (Figure 1D).

FREQUENCY OF TIM-3+T CELLS IN DIFFERENT DISEASE SUBGROUPS

We further analyzed the proportions of Tim-3+T cells in various subsets in the peripheral blood of healthy controls, patients with mild-to-moderate and severe COVID-19(Figure 2A). The results revealed that compared to the HC group, patients with COVID-19 showed a significant increase in the proportions of Tim-3+CD4+T cells and Tim-3+memory CD4+T cells, while Tim-3+naive CD4+T cells were significantly increased only in patients with mild-to-moderate COVID-19 (Figure 2B). The proportions of Tim-3+CD8+T cells, Tim-3+memory $CD8^+$ T cells, and Tim-3+naive CD8+T cells were all significantly increased in patients with COVID-19 compared to the HC group (Figure 2C). Furthermore, we observed a significant increase in the proportion of Tim-3+CD19+B cells in patients with mild-to-moderate COVID-19, while Tim-3+ASCs cells were significantly decreased (Figures S2B and S2D).

We analyzed the proportions of Tim-3+T lymphocyte subsets in peripheral blood among healthy controls, patients with T1D,

Table 2. Characteristics of healthy control and patients with different types of diabetes recruited into the study

Characteristics	Healthy Control	T1D	T2D	*p* value between groups
Number	36	10	35	
Age (year)	48.4 ± 18.9	36.1 ± 11.2	58.5 ± 12.9	
Male (n, %)	13(36.1%)	7(70.0%)	16(45.7%)	0.08
HbA1c (%)	5.7 ± 0.6	9.8 ± 3.2$^{###}$	9.2 ± 2.7$^{###}$	<0.001***
FBG (mmol/L)	4.9 ± 1.1	8.4 ± 3.1$^{#}$	9.1 ± 4.0$^{###}$	<0.001***
Leukocyte count (×10^9/L)	7.2 ± 3.0	5.8 ± 1.9	7.5 ± 2.8	0.326
Hemoglobin (g/L)	120.5 ± 21.5	127.4 ± 23.5	122.9 ± 19.9	0.711
Erythrocyte count (×10^{12}/L)	4.2 ± 0.6	4.2 ± 0.8	4.1 ± 0.7	0.926
Platelet count (×10^9/L)	223.6 ± 62.2	210.6 ± 77.7	237.3 ± 77.2	0.610
Neutrophil count (×10^9/L)	3.8 ± 3.2	2.9 ± 2.3	3.7 ± 2.5	0.717
Neutrophil percentage (%)	65.7 ± 8.7	64.8 ± 5.6	69.8 ± 11.2	0.203
Lymphocyte count (×10^9/L)	1.7 ± 0.6	1.5 ± 0.5	1.6 ± 0.7	0.528
Lymphocyte percentage (%)	26.0 ± 7.7	26.0 ± 5.4	23.0 ± 10.3	0.402
Monocyte count (×10^9/L)	0.4 ± 0.2	0.4 ± 0.1	0.4 ± 0.2	0.88
Monocyte percentage (%)	6.4 ± 2.0	7.5 ± 1.6	5.7 ± 1.5^{+}	0.039*
CRP (mg/L)	1.4 ± 1.2	2.9 ± 2.3	4.0 ± 4.0	0.223
D-dimer (μg/mL)	0.4 ± 0.2	0.4 ± 0.3	0.8 ± 0.9	0.149
TG (mmol/L)	1.3 ± 0.8	1.8 ± 1.3	1.9 ± 1.2	0.130
TC (mmol/L)	4.2 ± 1.0	5.1 ± 1.5	4.8 ± 1.2	0.099
HDL-C (mmol/L)	1.1 ± 0.4	0.9 ± 0.3	1.0 ± 0.3	0.228
LDL-C (mmol/L)	2.7 ± 0.9	3.8 ± 1.5$^{#}$	3.1 ± 0.9	0.034*
ALT (U/L)	18.0 ± 10.3	24.1 ± 9.92	31.0 ± 25.2	0.060
AST (U/L)	19.0 ± 7.2	22.0 ± 8.9	23.8 ± 15.3	0.356
TBIL (μmol/L)	8.5 ± 3.0	10.7 ± 2.5	9.4 ± 3.3	0.248
DBIL (μmol/L)	3.1 ± 1.2	3.4 ± 0.8	3.3 ± 1.4	0.777
CR (μmol/L)	63.7 ± 16.2	67.9 ± 9.5	83.5 ± 51.5	0.116
UA (μmol/L)	265.3 ± 116.1	267.2 ± 82.4	317.7 ± 141.1	0.238
25-hydroxyl-VitaminD (nmol/L)	48.4 ± 16.4	37.4 ± 8.4	46.3 ± 18.6	0.279

Data are expressed as the mean ± standard deviation for qualitative data.
PCT, procalcitonin; ESR, erythrocyte sedimentation rate; CRP means C-reactive protein.
TG, triglyceride; TC, total cholesterol; HDL-C, high density lipid-cholesterol; LDL-C, low density lipid-cholesterol; ALT, alanine aminotransferase; AST, aspartate transaminase; TBIL, total bilirubin; DBIL, conjugated bilirubin; CR, creatinine; UA, uric acid; FBG, fasting blood glucose.
Differences between groups: *$p < 0.05$, ***$p < 0.001$.
In comparison with healthy control: $^{#}p < 0.05$, $^{###}p < 0.001$.

and T2D (Figure 3A). The results showed that patients with T1D had significantly lower proportions of Tim-3+CD4$^+$ and CD8+T cells, with no significant differences found in memory T cells and naive T cells (Figures 3B and 3C). Patients with T2D exhibited a higher proportion of Tim-3+naive CD8+T cells compared to the healthy control group (Figure 3C).

We also analyzed the proportions of Tim-3+lymphocyte subsets in peripheral blood among patients with COVID-19 and patients with COVID-19 combined with T1D or T2D (Figure 4A). The results showed that in patients with COVID-19 combined with T1D, the proportions of Tim-3+CD4+T cells were lower than in patients with COVID-19 (Figure 4B). Additionally, compared to patients with COVID-19 combined with T2D, patients with COVID-19 combined with T1D had decreased proportions of Tim-3+CD8+T cells (Figure 4C). No other significant differences were found. In CD4 and CD8$^+$ T cells, we also observed an increase in the co-expression of inhibitory receptors with Tim-3 (Figures S5B–S5D).

FUNCTIONAL STATUS OF CD4$^+$ AND CD8+Tim+ T CELLS

Then, we compared the proliferation, activation, and cytokine secretion abilities of Tim-3+ T cells and Tim-3- T cells in mice. To increase the proportion of Tim-3+ T cells, we cultured mouse spleen cells for 3 days under stimulation with anti-CD3, anti-CD28, and IL-12. Cells were then collected for flow cytometry analysis. Functional experiments in mice showed that, compared to Tim-3- CD4$^+$ T cells, a lower proportion of Tim-3+ CD4$^+$ T cells expressed CD25, CD69, and Ki-67 (Figures 5A and 5B). However, a higher proportion of Tim-3+ CD4$^+$ T cells produced IFN-γ and TNF-α (Figure 5C). Similar findings were observed in the mouse CD8$^+$ T cell subset, where Tim-3+ CD8$^+$ T cells showed a lower proportion of cells expressing CD25, CD69, and Ki-67 (Figures 6A and 6B), while a higher proportion of cells produced granzyme B (GZMB), TNF-α, and IFN-γ (Figure 6C). We observed consistent results in healthy individuals (Figure S5A).

Table 3. Characteristics of patients with COVID-19 alone and patients with COVID-19 with different types of diabetes recruited into the study

Characteristics	COVID-19 alone	COVID-19 with T1D	COVID-19 with T2D	*p* value between groups
Number	42	11	52	
Age (years)	69.1 ± 14.3	48.1 ± 18.9	66.0 ± 15.1	
Male (n,%)	21(50.0%)	9(81.8%)	35(67.3%)	0.2
Leukocyte count ($\times10^9$/L)	7.3 ± 2.6	9.4 ± 4.1	7.7 ± 3.4	0.2
Hemoglobin (g/L)	119.5 ± 19.4	124.3 ± 20.2	111.7 ± 26.1	0.178
Erythrocyte count ($\times10^{12}$/L)	4.0 ± 0.7	4.1 ± 0.8	3.8 ± 0.8	0.477
Platelet count ($\times10^9$/L)	260.0 ± 103.5	245.3 ± 74.2	229.7 ± 112.7	0.475
Neutrophil count ($\times10^9$/L)	2.4 ± 3.2	5.6 ± 5.3	4.2 ± 3.9	0.035*
Neutrophil percentage (%)	73.0 ± 12.3	73.8 ± 12.6	74.7 ± 13.5	0.844
Lymphocyte count ($\times10^9$/L)	1.3 ± 0.8	1.4 ± 0.7	1.2 ± 0.7	0.689
Lymphocyte percentage (%)	18.2 ± 11.2	18.2 ± 10.6	18.0 ± 11.8	0.995
Monocyte count ($\times10^9$/L)	0.6 ± 0.5	0.6 ± 0.2	0.4 ± 0.2	0.13
Monocyte percentage (%)	7.3 ± 3.6	6.6 ± 2.4	5.8 ± 1.7	0.053
Lactic acid (mmol/L)	2.8 ± 1.3	2.2 ± 0.5	2.6 ± 0.7	0.486
CRP (mg/L)	29.3 ± 39.7	35.4 ± 41.6	32.8 ± 37.8	0.917
IL-6 (ng/mL)	12.8 ± 14.4	35.2 ± 22.7	29.1 ± 33.2	0.198
D-dimer (μg/mL)	1.1 ± 1.1	1.3 ± 1.5	1.2 ± 0.9	0.842
TG (mmol/L)	1.6 ± 1.0	2.0 ± 1.8	1.9 ± 1.8	0.656
HDL-C (mmol/L)	1.0 ± 0.3	1.0 ± 0.3	0.9 ± 0.3	0.221
LDL-C (mmol/L)	2.7 ± 0.8	3.3 ± 1.4	2.3 ± 0.9^{+}	0.015*
ALT (U/L)	34.0 ± 21.1	36.4 ± 35.0	33.6 ± 27.4	0.951
AST (U/L)	32.1 ± 15.7	35.0 ± 34.4	32.4 ± 11.8	0.903
TBIL (μmol/L)	9.4 ± 4.0	10.0 ± 5.2	10.6 ± 6.8	0.657
DBIL (μmol/L)	3.8 ± 2.1	4.5 ± 3.6	4.6 ± 3.2	0.471
BUN (mmol/L)	4.9 ± 1.7	5.9 ± 2.3	10.2 ± 7.7$^{\#\#}$	0.007**
UA (μmol/L)	222.2 ± 111.9	256.5 ± 151.2	292.8 ± 104.2	0.052
25-hydroxyl-VitaminD (nmol/L)	43.3 ± 16.5	50.7 ± 20.9	45.5 ± 18.8	0.636
HbA1c (%)	6.0 ± 0.4	9.7 ± 2.6$^{\#\#\#\#}$	8.5 ± 1.7$^{\#\#\#}$	<0.0001****
FBG (mmol/L)	5.3 ± 0.9	8.1 ± 3.3	9.6 ± 4.3$^{\#\#}$	0.003**

Data are expressed as the mean ± standard deviation for qualitative data.
PCT, procalcitonin; ESR, erythrocyte sedimentation rate; CRP means C-reactive protein.
TG, triglyceride; TC, total cholesterol; HDL-C, high density lipid-cholesterol; LDL-C, low density lipid-cholesterol; ALT, alanine aminotransferase; AST, aspartate transaminase; TBIL, total bilirubin; DBIL, conjugated bilirubin; CR, creatinine; UA, uric acid; FBG, fasting blood glucose.
Differences between groups: $^{*}p < 0.05$, $^{**}p < 0.01$, $^{****}p < 0.0001$.
In comparison with patients with COVID-19 alone: $^{\#\#}p < 0.01$, $^{\#\#\#}p < 0.001$, $^{\#\#\#\#}p < 0.0001$.

DOWNREGULATION OF THE JAK/STAT SIGNAL PATHWAY IN MOUSE TIM-3+ T CELLS

We continued to explore the molecular mechanisms of Tim-3+T cells. We performed RNA-seq analysis of differentially expressed genes by sorting mouse Tim-3+T cells and Tim-3-T cells using flow cytometry. We recognized 185 up-regulated genes and 332 down-regulated genes as the differentially expressed genes (Figure 7A). Gene Ontology (GO) analysis revealed that the genes relating to ''immune response'' and ''immune system process'' were enriched in the Tim-3+T cells, compared with the Tim-3-T cells (Figure 7B). Kyoto Encyclopedia of Genes and Genomes (KEGG) analysis showed that ''JAK-STAT signaling pathway'' was enriched in the Tim-3+T cells (Figure 7C). Further analysis revealed that genes in the JAK-STAT signaling pathway were significantly downregulated in Tim-3+T cells. Additionally, our results showed that *Ifng* and *Gzmb* genes were significantly upregulated in Tim-3+CD4^{+} T cells (Figure 7D).

DOWNREGULATION OF THE JAK/STAT SIGNAL PATHWAY IN TIM-3+ T CELLS UNDER DISEASE CONDITIONS

To better study the function of Tim-3+ T cells in an exhausted state, we used an *in vitro* model of chronic T cell stimulation as described by Mirko Corselli et al.,[30] along with the NOD mouse disease model. In which mouse spleen cells were continuously

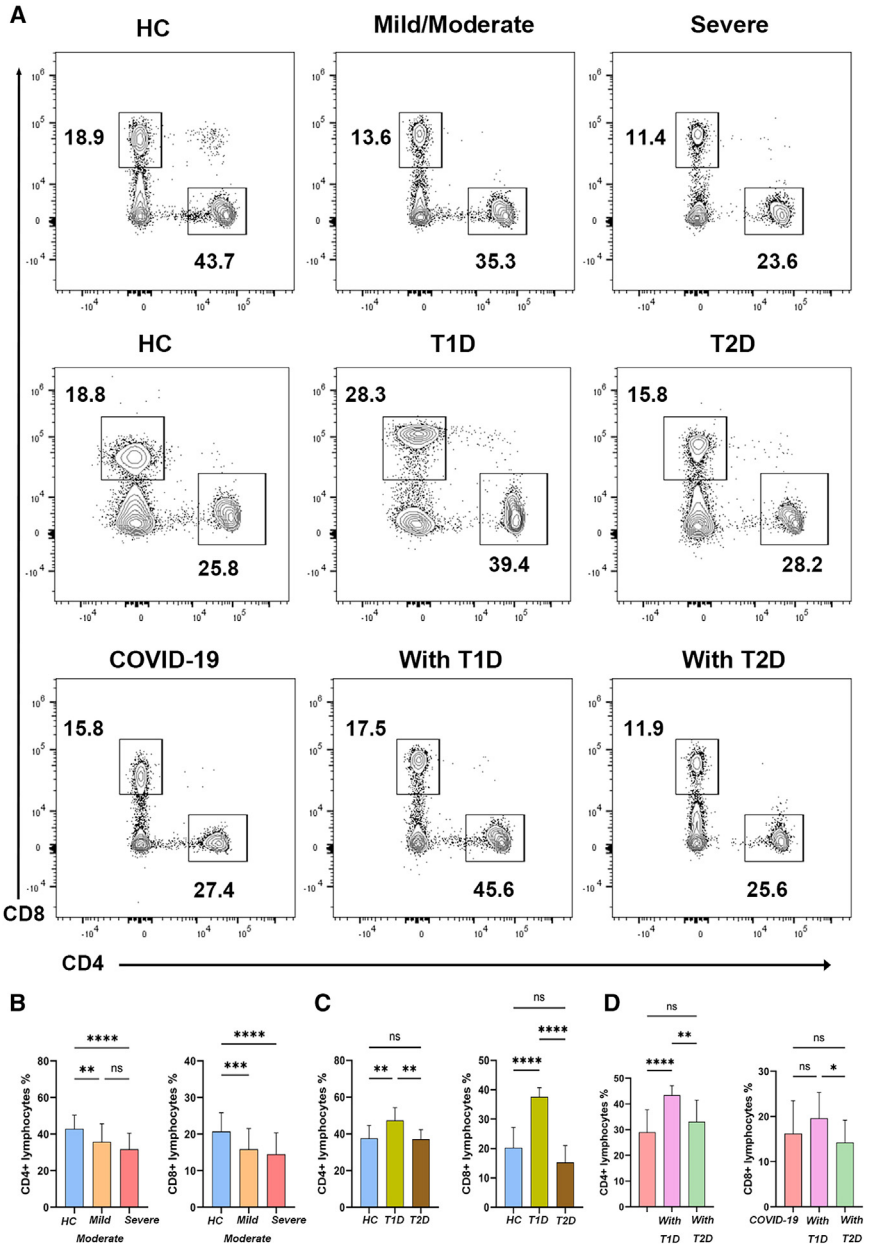

Figure 1. Proportions of various T cell subsets in the peripheral blood of healthy controls, patients with COVID-19, and diabetes

(A) Flow cytometry plots representing the proportions of CD4+T cell subsets and CD8+T cell subsets in the peripheral blood of healthy controls and patients with COVID-19 with different severities. T1D, T2D, and COVID-19 with T1D or T2D.

(B) Bar graphs representing the proportions of CD4+T cell subsets and CD8+T cell subsets in the peripheral blood of healthy controls and patients with COVID-19 with different severities. (36 healthy controls, 24 mild-to-moderate COVID-19 cases, 18 severe COVID-19 cases).

(C) Bar graphs representing the proportions of CD4+T cell subsets and CD8+T cell subsets in the peripheral blood of HC, T1D, and T2D. (36 healthy controls, 10 patients with T1D, 35 patients with T2D).

(D) Bar graphs representing the proportions of CD4+T cell subsets and CD8+T cell subsets in the peripheral blood of COVID-19 alone, COVID-19 with T1D, and COVID-19 with T2D. (42 patients with COVID-19 alone, 11 patients with COVID-19 with T1D, 52 patients with COVID-19 with T2D). (*$p < 0.05$, **$p < 0.01$, ***$p < 0.001$, ****$p < 0.0001$).

stimulated with IL-2 and αCD3/CD28 for 14 days to induce chronic stimulation. Cells were collected on days 0, 3, 7, and 14 for flow cytometry analysis. We analyzed the expression levels of Tim-3 on $CD3^+$ T cells at each time point, and results showed that the percentage of Tim-3+ T cells gradually increased over time (Figure 8A). Since Tim-3 expression on T cells was low on day 0, we focused on analyzing the functional state of Tim-3+ T cells on days 3, 7, and 14 of stimulation. We found that after 7 and 14 days of stimulation, Tim-3+ T cells showed impaired activation, proliferation, and cytokine secretion capacity (Figure 8B). In NOD mice with spontaneous diabetes, we found that, compared to Tim-3- T cells, Tim-3+ T cells exhibit inhibited activation, proliferation, and cytokine expression (Figure 8C). In CD3+Tim-3+ T cells from NOD mice, we found reduced expression levels of JAK/STAT pathway-related genes through RT-qPCR (Figure 8D).

We also measured the mRNA expression levels of JAK/STAT pathway-related genes in circulating Tim-3+ T cells from healthy controls (HC), patients with COVID-19, patients with type 1 diabetes (T1D), and patients with both COVID-19 and T1D. The results showed that, compared to Tim-3- T cells, the expression levels of JAK-STAT pathway-related genes *JAK1*, *STAT1*, and *STAT2* were reduced in Tim-3+ T cells from HC, COVID-19, T1D, and COVID-19 with patients with T1D (Figure 8E). We also measured the expression levels of IFN-γ, TNF-α, and GZMB in Tim-3+ T cells from healthy controls (HC), patients with COVID-19, patients with T1D , and patients with both COVID-19 and T1D. The results showed increased expression levels of IFN-γ, TNF-α, and GZMB in Tim-3+ T cells from healthy controls, whereas in Tim-3+ T cells from COVID-19, T1D, and COVID-19 with patients with T1D, the expression levels of IFN-γ, TNF-α, and GZMB were reduced (Figure 8F).

DISCUSSION

In this study, we evaluated changes in peripheral blood lymphocytes of patients with COVID-19 and diabetes and further analyzed the proportion of Tim-3+T cells. We found an increased

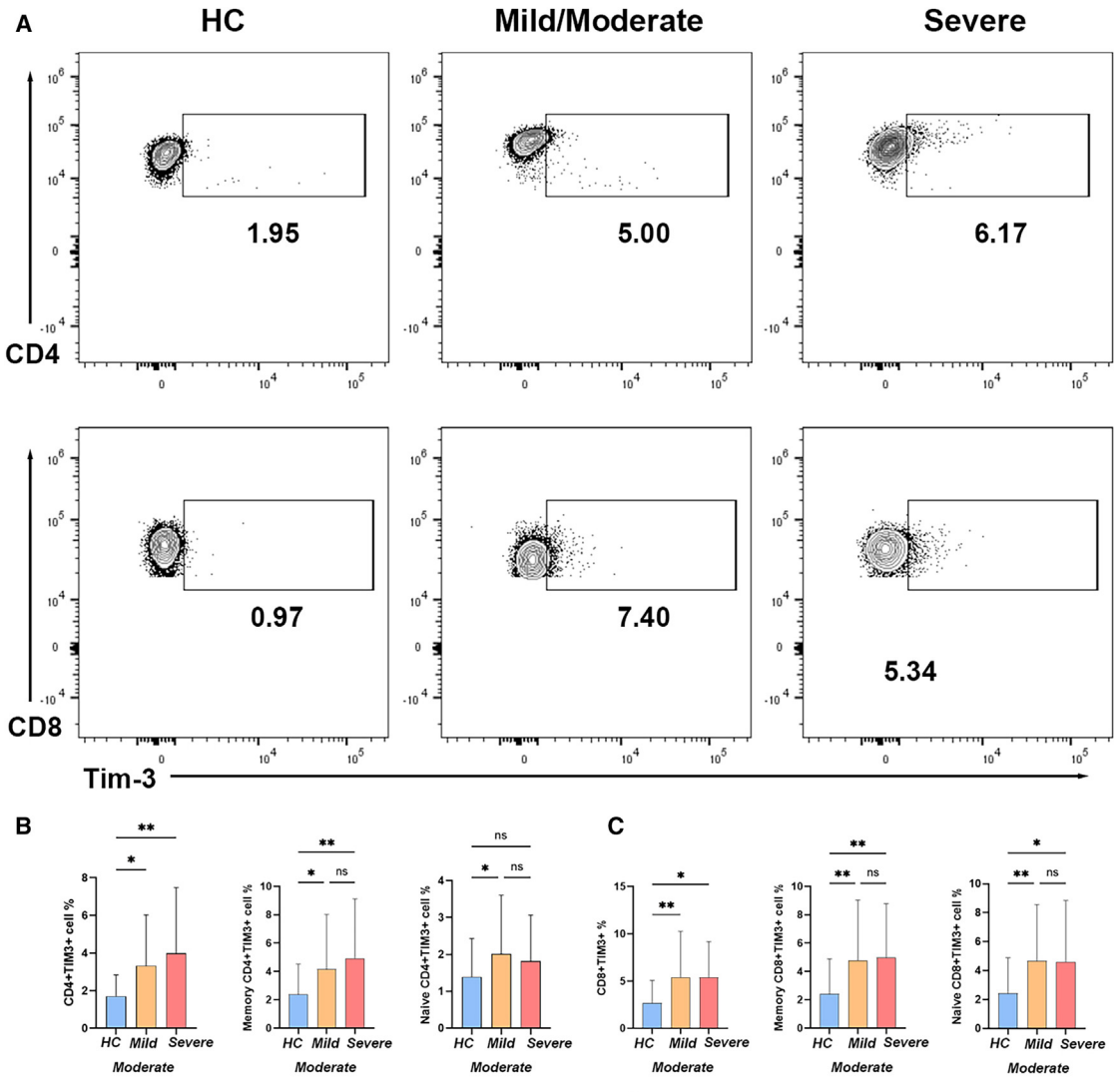

Figure 2. Increased frequency of Tim-3+T cell subsets in COVID-19 with different severities

(A) Flow cytometry was performed to detect the proportions of Tim-3+CD4+T and CD8+T in the peripheral blood of healthy controls and patients with COVID-19 with different severities.

(B and C) Statistical analysis of Tim-3+CD4+T cell and CD8+T cell subsets from Healthy Control (n = 36), patients with mild-to-moderate COVID-19 (n = 24), patients with severe COVID-19 (n = 18). (*p < 0.05, **p < 0.01).

proportion of Tim-3+T cells in patients with COVID-19, while a significant decrease was observed in patients with T1D . Additionally, the proportion of Tim-3+T cells in patients with both COVID-19 and T1D also decreased. Our analysis characterizes Tim-3+ T cell alterations in patients with concurrent COVID-19 and diabetes. Additionally, we found that Tim-3+ T cells exhibit inhibited proliferation and activation, along with altered cytokine secretion. Through mouse RNA-seq analysis, we identified the JAK/STAT pathway, which may be associated with the role of Tim-3+ T cells in immune regulation. We also observed reduced expression levels of JAK/STAT pathway-related genes in Tim-3+ T cells from both healthy individuals and patients. In summary, our study provides mechanistic insights into the immunoregulatory role of Tim-3+ T cells in COVID-19 and T1D.

T cell exhaustion is a state of T cell dysfunction characterized by impaired effector function, sustained expression of inhibitory receptors, and transcriptional states distinct from functional effector or memory T cells.[31,32] Our findings expand on the research by Avery et al.,[33] who suggested that Tim-3 might promote T cell exhaustion by limiting the memory T cell pool and enhancing the production of activated and short-lived effector cells. These pieces of evidence reflect the complexity of Tim-3-mediated immune regulation. A deeper investigation into the functional impairment of various peripheral blood T cells in patients with COVID-19 and diabetes is of great significance.

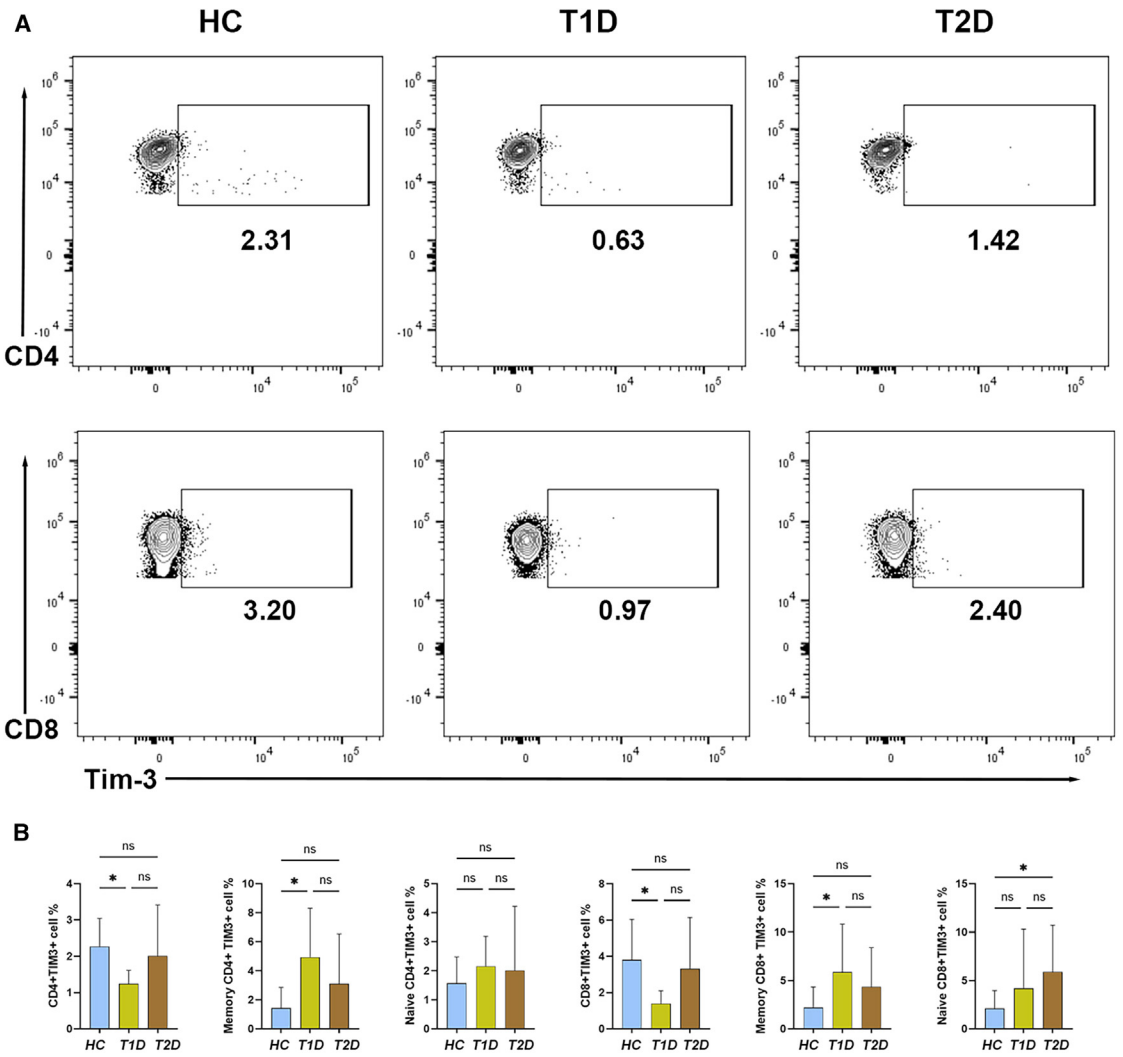

Figure 3. Decreased frequency of Tim-3+T cell subsets in HC, T1D and T2D

(A) Flow cytometry was performed to detect the proportions of Tim-3+CD4+T and CD8+T in the peripheral blood of healthy controls, T1D and T2D.

(B and C) Statistical analysis of Tim-3+CD4+T cell and CD8+T cell subsets from Healthy Control (n = 36), patients with T1D (n = 10), patients with T2D (n = 35). (*p < 0.05).

As a highly contagious disease, COVID-19 has rapidly spread and contributed to the epidemic status of non-communicable diseases such as diabetes. Likewise, diabetes also impacts the occurrence and prognosis of COVID-19, indicating a close interplay between these two diseases. However, the immunological mechanisms underlying the co-occurrence of these two diseases are still poorly understood. Our study examined the frequencies of lymphocyte subsets and Tim-3+ T cells in peripheral blood from patients with COVID-19 with different diabetes subtypes. Compared to patients solely infected with COVID-19, those with combined T1D and COVID-19 showed a significant increase in CD4+T cells and a slight increase in CD8+T cells. However, the Tim-3+CD4+T cell subset exhibited a significant decrease, while the decrease in the Tim-3+CD8+T cell subset was not significant. A recent study found higher Tim-3+CD4+T cells in patients with T1D during the remission phase compared with progression. The decreased Tim-3+T cells in patients with T1D suggests insufficient immune regulation, which might be involved in the pathogenesis of T1D.[21] In the context of T1D, we observed a decrease in Tim-3+ T cells in patients with COVID-19, which may lead to excessive T cell activation, contributing to T cell immune dysregulation and promoting the generation of autoimmune T cells alongside other factors. However, these autoimmune T cells do not exhibit antiviral activity.

Previous studies have reported that Tim-3+T cells can produce higher levels of pro-inflammatory cytokines such as IFN-γ and TNF-α.[34–36] There are also studies reporting reduced levels of pro-inflammatory cytokines. In our *in vitro* study simulating the chronic stimulation of T cells, we observed that, during the early phase of stimulation, Tim-3+ T cells exhibited impaired activation and proliferation alongside increased cytokine expression. However, as stimulation time was extended, we

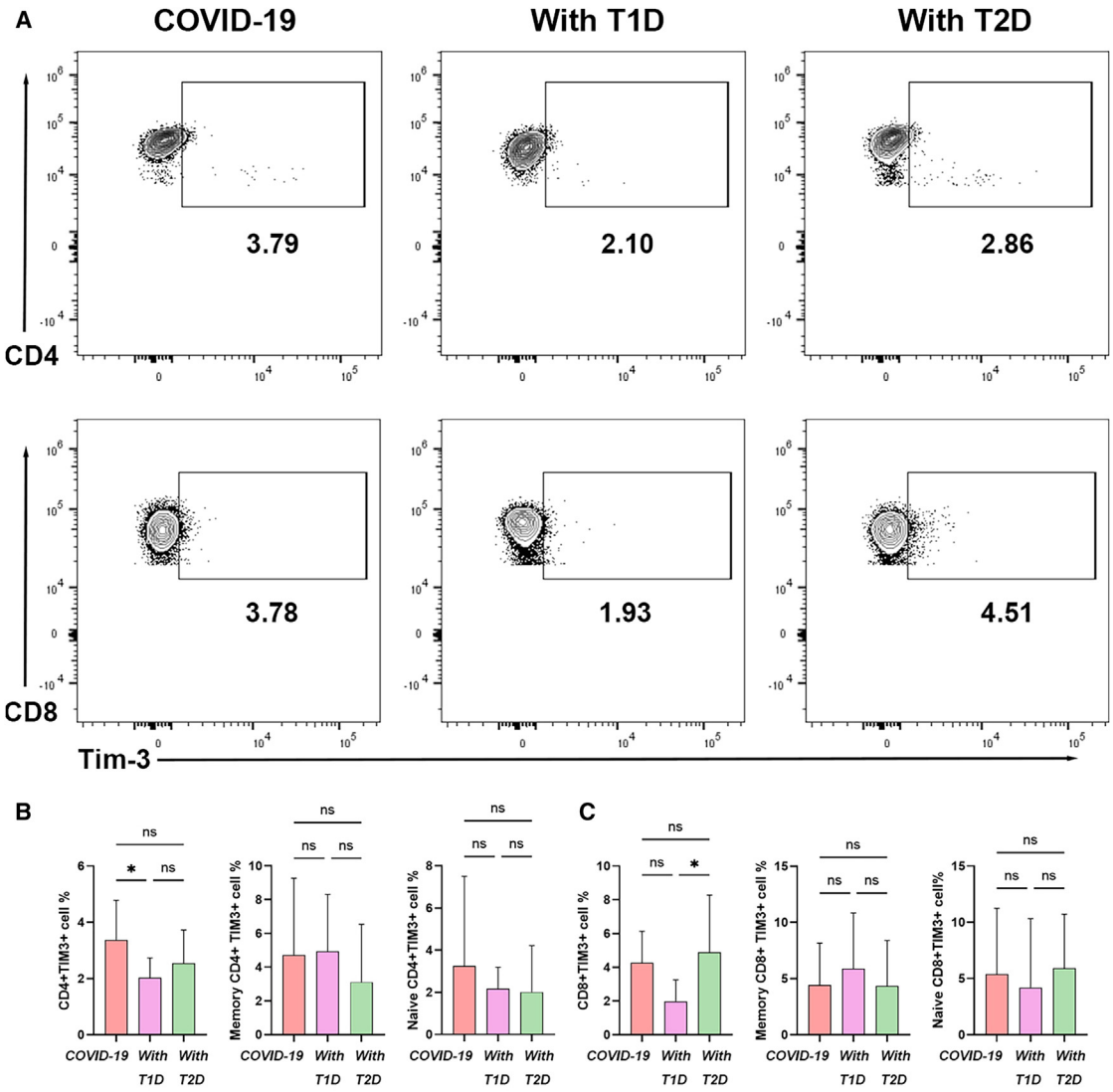

Figure 4. Decreased frequency of Tim-3+T cell subsets in patients with COVID-19, patients with COVID-19 with T1D or T2D

(A) Flow cytometry was performed to detect the proportions of Tim-3+CD4+T and CD8+T in the peripheral blood of patients with COVID-19, patients with COVID-19 with T1D or T2D.

(B and C) Statistical analysis of Tim-3+CD4+T cell and CD8+T cell subsets from patients with COVID-19 (n = 42), patients with COVID-19 with T1D (n = 11), patients with COVID-19 with T2D (n = 52). (*$p < 0.05$).

noted a decrease in cytokine expression in Tim-3+ T cells. Furthermore, we discovered that in NOD mice, the activation, proliferation, and cytokine expression of Tim-3+ T cells were all suppressed. Although the early phase of the model may not fully reflect the functional state of Tim-3+ T cells in disease conditions, our initial findings of impaired activation and proliferation in Tim-3+ T cells are consistent with observations in disease states, suggesting that the early stimulation phase provides valuable insights for research.

In this study, we propose that the functional changes in Tim-3+T cells may be related to the JAK/STAT signaling pathway. Our RNA-seq analysis revealed a significant enrichment of the JAK/STAT signaling pathway in Tim-3+T cells, with genes in the JAK/STAT pathway significantly downregulated in Tim-3+T cells. The JAK-STAT signaling pathway is an evolutionarily conserved signaling mode that enables cells to communicate with the external environment and drives a series of physiological and pathological processes, including cell proliferation, metabolic regulation, immune response, inflammation, and tumor occurrence.[37,38] The dysregulation of the JAK/STAT pathway is associated with various diseases.[39,40] In T cells, the activation of the JAK/STAT signaling pathway promotes cell proliferation, differentiation, and functional expression.[41,42] We found decreased expression levels of JAK/STAT pathway-related genes in Tim-3+ T cells from both healthy individuals and patients. Although our RNA-seq utilized splenocytes from mice

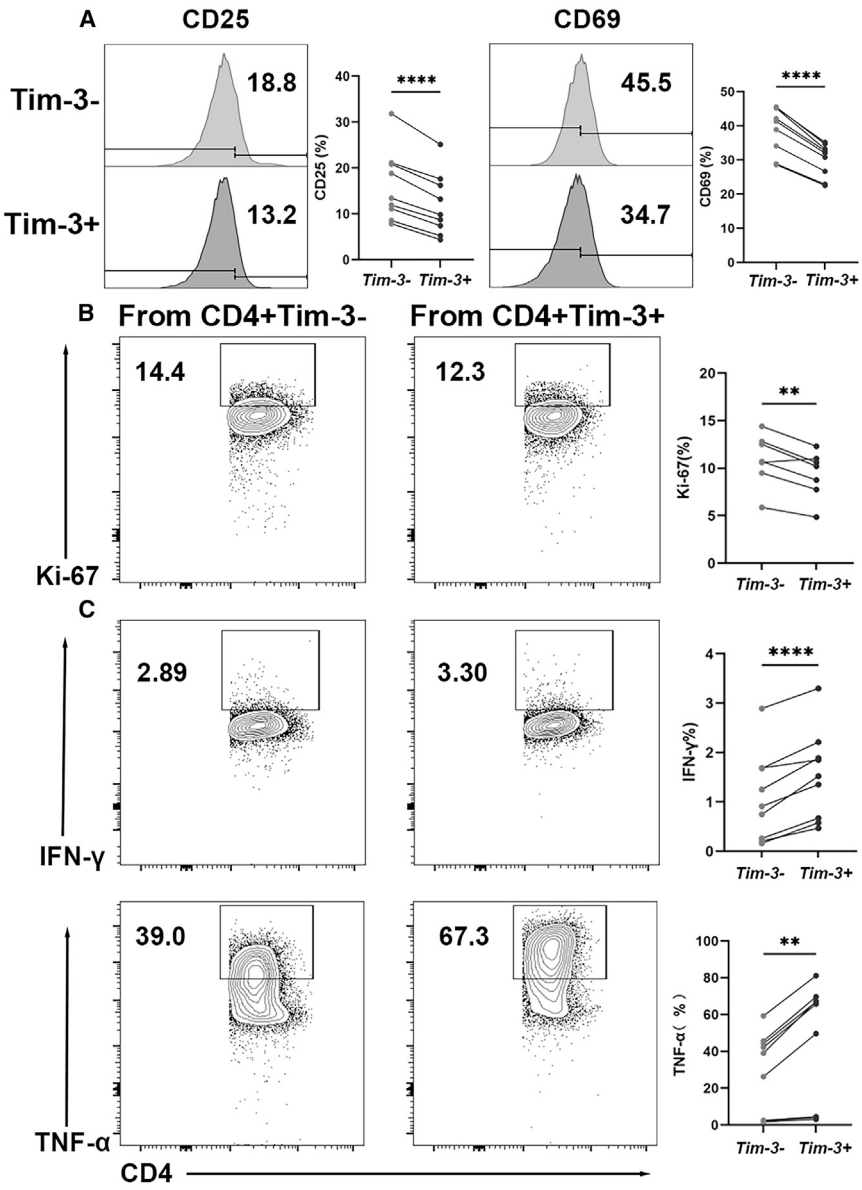

Figure 5. In the early stages of stimulation, mouse Tim-3+CD4+T cell subsets exhibited low activation, low proliferation, and high pro-inflammatory cytokine secretion capacity

(A) Flow cytometry gating and statistical analysis were conducted to analyze the expression frequency of activation markers, including CD25 and CD69, in Tim-3+CD4+T cells and Tim-3-CD4+T cells.

(B) Flow cytometry gating and statistical analysis were performed to analyze the proliferation marker Ki-67 in Tim-3+CD4+T cells and Tim-3-CD4+T cells.

(C) Flow cytometry gating and statistical analysis were conducted to analyze the frequency of pro-inflammatory cytokine secretion, including IFN-γ and TNF-α, in Tim-3+CD4+T cells and Tim-3-CD4+T cells. ($n = 9$, $^{**}p < 0.01$, $^{****}p < 0.0001$).

prior to stimulation and may not fully reflect the mechanisms of Tim-3+ T cells in disease states, the observed changes in the JAK/STAT pathway within Tim-3+ T cells hold biological significance for their immunoregulatory role.

We observed consistent results of inhibited proliferation and activation in Tim-3+ T cells in both mouse and human T cell functions. Although our RNA-seq analysis was conducted on early-stimulated splenocytes from mice, we also detected the downregulation of JAK/STAT pathway-related gene expression in Tim-3+ T cells from both healthy individuals and patients. This conserved pathway may play a key role in the immunoregulatory functions of Tim-3+ T cells.

In summary, our study identifies a Tim-3+ T cell-mediated immunoregulatory pathway that may contribute to the pathogenesis of COVID-19 and T1D, providing potential implications for clinical management.

Limitations of the study

Our study has several limitations. First, the observed changes in the Tim-3+ T cell subset were based on a relatively small patient cohort, which may affect the generalizability of the results. Validation in a larger cohort is needed to strengthen the robustness of these findings. Second, due to the limited sample size, we could not perform viral subtype analysis in patients with COVID-19-infected . Since different SARS-CoV-2 subtypes may elicit distinct immune responses, the absence of this data limits our understanding of Tim-3+ T cell subset dynamics. Future studies analyzing different viral variants could provide more detailed insights. Importantly, our RNA-seq analysis used cells from normal mice and identified the downregulation of the JAK/STAT pathway in Tim-3+ T cells, which may not fully reflect disease states. We validated this finding via RT-qPCR in NOD mice and patients' samples, with consistent results. This suggests a potential role for the JAK/STAT pathway in disease progression, but its precise function and mechanism warrant further investigation.

RESOURCE AVAILABILITY

Lead contact

Further information and requests for resources and reagents should be directed to and will be fulfilled by the lead contact, Bin Zhao (binzhao@csu.edu.cn; bin.zhao@live.com).

Materials availability

This study did not generate new unique reagents.

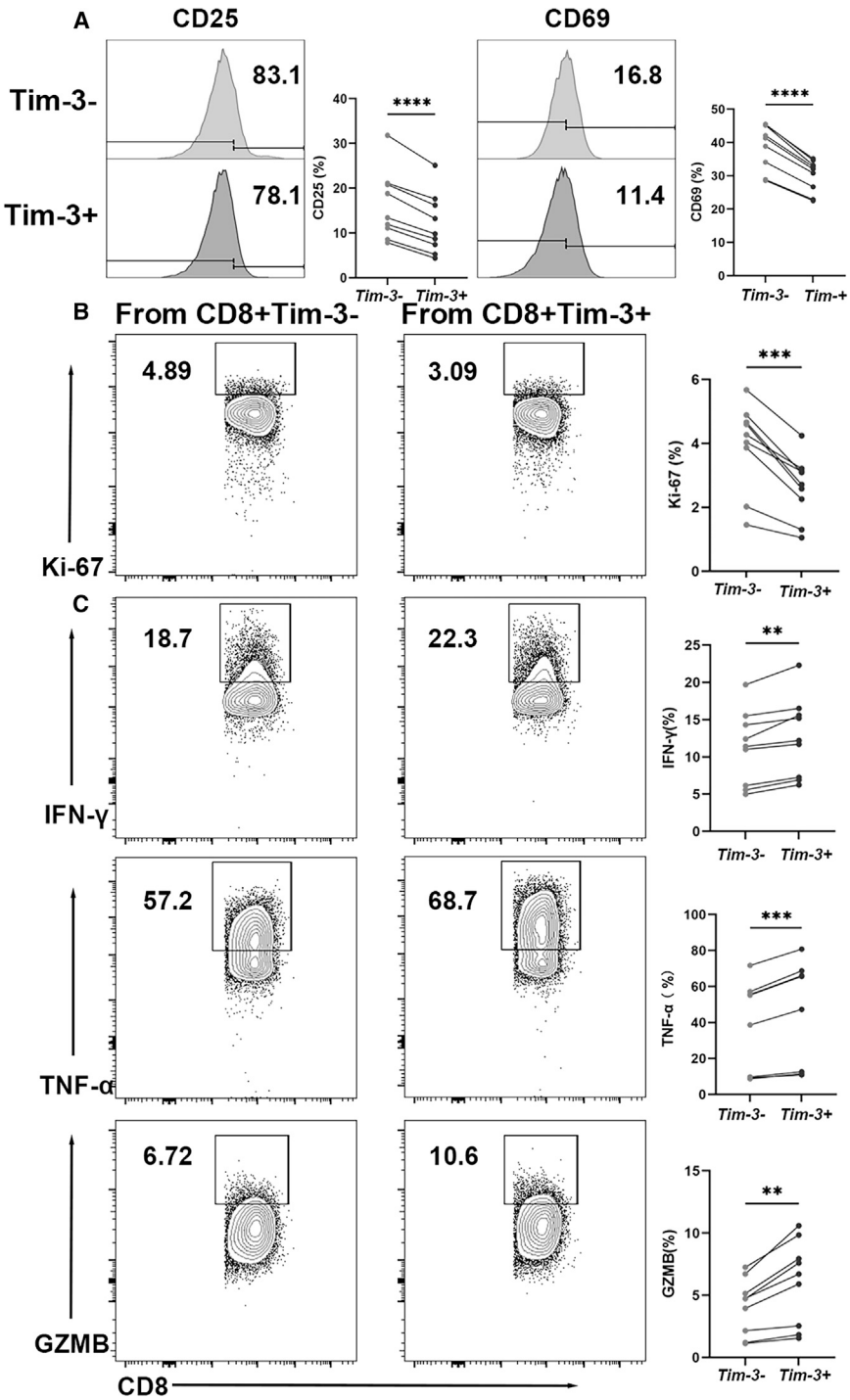

Figure 6. In the early stages of stimulation, mouse Tim-3+CD8+T cell subsets exhibited low activation, low proliferation, and high pro-inflammatory cytokine secretion capacity

(A) Flow cytometry gating and statistical analysis were conducted to analyze the expression frequency of activation markers, including CD25 and CD69, in Tim-3+CD8+T cells and Tim-3-CD8+T cells.

(B) Flow cytometry gating and statistical analysis were performed to analyze the proliferation marker Ki-67 in Tim-3+CD8+T cells and Tim-3-CD8+T cells.

(C) Flow cytometry gating and statistical analysis were conducted to analyze the frequency of pro-inflammatory cytokine secretion, including IFN-γ, TNF-α, and Granzyme B, in Tim-3+CD8+T cells and Tim-3-CD8+T cells. (n = 9, $^{**}p < 0.01$, $^{***}p < 0.001$, $^{****}p < 0.0001$).

Data and code availability

- All RNA-seq data have been deposited at Mendeley data (https://doi.org/10.17632/94r6y9jb6g.1, https://doi.org/10.17632/zzf3x4gs24.1, https://doi.org/10.17632/hpmd99x5fn.1, https://doi.org/10.17632/rc63wxj24n.1, https://doi.org/10.17632/vhpkwzgtrm.1, https://doi.org/10.17632/vrvzgf6z69.1, https://doi.org/10.17632/r34jcp2pbr.1).
- This study does not report any original code.
- Any additional information required to reanalyze the data reported in this article is available from the lead contact upon request.

ACKNOWLEDGMENTS

This study was supported by the Noncommunicable Chronic Diseases-National Science and Technology Major Project (2023ZD0507300,

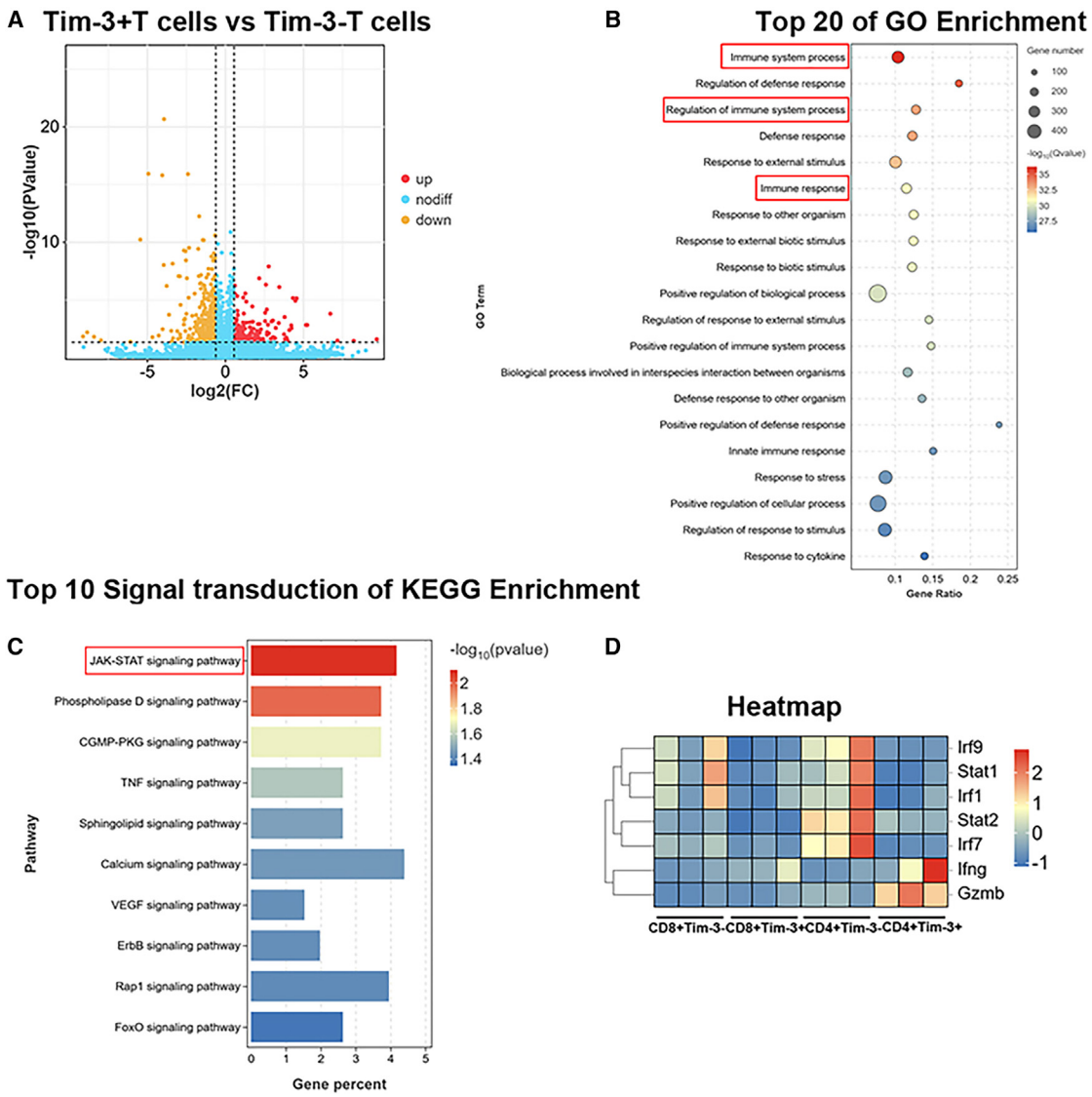

Figure 7. Downregulation of the JAK/STAT Signal pathway in mouse Tim-3+T cells

(A) The volcano plot illustrated the differentially expressed genes in Tim-3+T cells compared to Tim-3-T cells, in which genes significantly upregulated were shown in red, genes that significantly downregulated were shown in yellow, and other genes were shown in blue. Each gene was symbol-coded according to its adjusted p value generated using DESeq2 with a Benjamini-Hochberg false discovery rate (FDR) correction. The cutoff values were recognized as adjusted $p < 0.05$ and fold change >1.5.

(B) Functional annotation analysis with the top 20 enrichment Gene Ontology (GO) terms were shown.

(C)Signal transduction analysis with the top 10 enrichment Kyoto Encyclopedia of Genes and Genomes (KEGG) pathway.

(D) Heatmap displaying for JAK/STAT signal pathway associated genes in Tim-3+T cells compared to Tim-3-T cells.

2023ZD0507303),the National Natural Science Foundation of China (grant no. 82170795 and 82470814), the Natural Science Foundation of Hunan Province (grant no. 2023JJ30805), the Scientific Research Program of FuRong Laboratory (2024PT5105)and Central South University Research Programme of Advanced Interdisciplinary Studies (2023QYJC008). The graphical abstract was created By Figdraw (https://www.figdraw.com).

AUTHOR CONTRIBUTIONS

SYW, BZ, WJL, and MJZ designed the study, analyzed and interpreted data, and drafted the article. WJL, MJZ, and MYG conducted the experiments, acquired and analyzed data. SYW, BZ, and JQH discussed the results and revised the article. All authors have reviewed and approved the final version. SYW, BZ, WJL, and MJZ are responsible for the integrity of the work as a whole.

DECLARATION OF INTERESTS

The authors declare no competing interests.

STAR★METHODS

Detailed methods are provided in the online version of this paper and include the following:

- KEY RESOURCES TABLE
- EXPERIMENTAL MODEL AND STUDY PARTICIPANT DETAILS

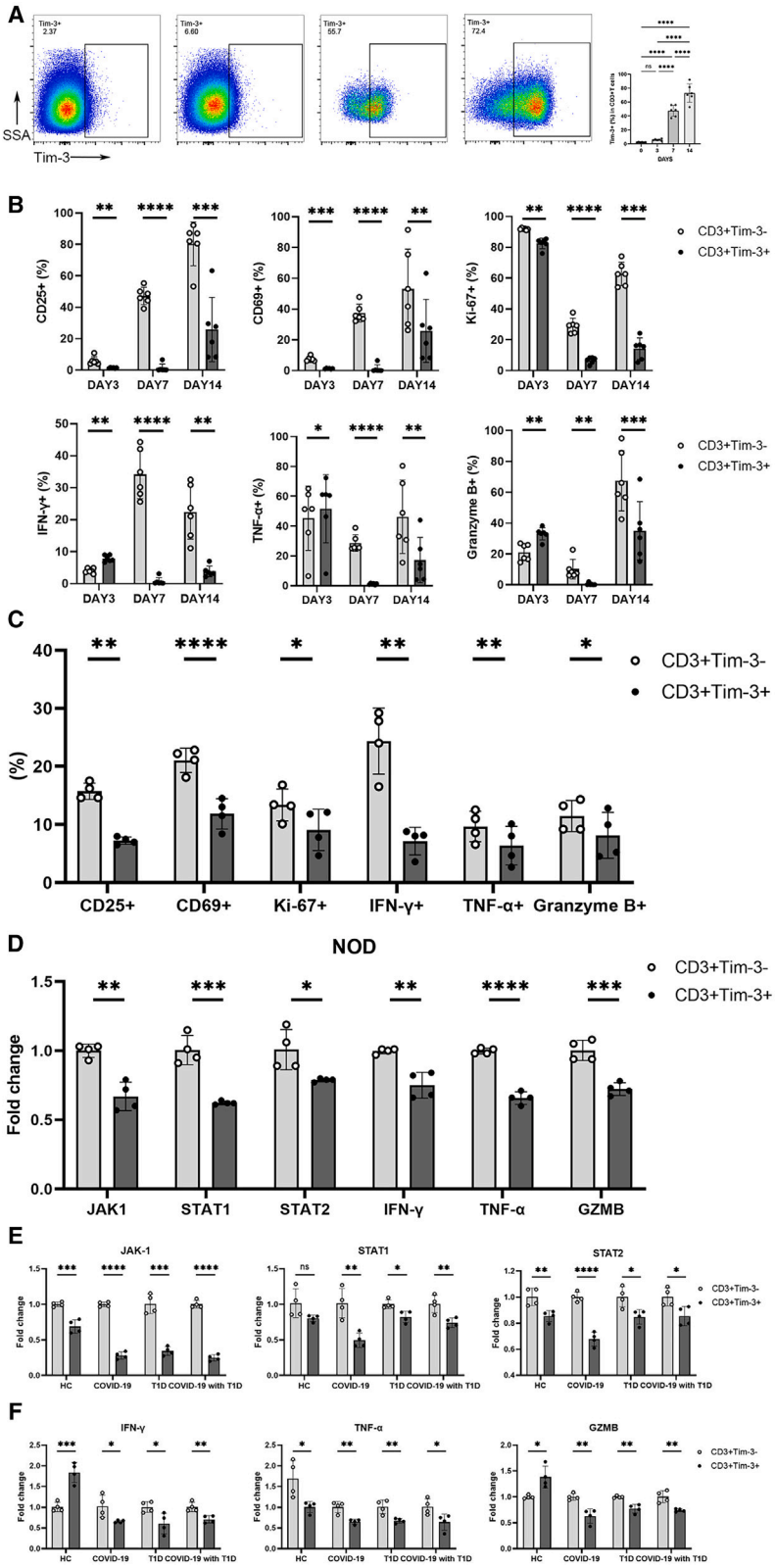

Figure 8. Functional and JAK/STAT Pathway Changes in Tim-3+ T Cells under disease conditions

(A) Flow cytometry plots and statistical graphs of Tim-3 expression levels on $CD3^+$ T cells from mouse spleen cells at different stimulation time points. (n = 6, $^{****}p < 0.0001$) (B) Statistical graphs of activation, proliferation, and cytokine levels of Tim-3+ T cells from mouse spleen cells at different stimulation time points. (n = 6, $^{*}p < 0.05$, $^{**}p < 0.01$, $^{***}p < 0.001$, $^{****}p < 0.0001$) (C) Statistical graphs of activation, proliferation, and cytokine levels in Tim-3+T and Tim-3-T cells in NOD mice. (n = 4, Horizontal bars represent the mean ± SD. $^{*}p < 0.05$, $^{**}p < 0.01$, $^{****}p < 0.0001$ by paired Student's t test.) (D) Quantitative real-time PCR (qPCR) analysis for JAK1, STAT1, STAT2, IFN-γ, TNF-α and GZMB expression from CD3+Tim-3+T cells in NOD mouse (n = 4) (E) Quantitative real-time PCR (qPCR) analysis for JAK1, STAT1 and STAT2 expression from CD3+Tim-3+T cells in Healthy control (n = 4), COVID-19 (n = 4), patients with T1D (n = 4), and patients with COVID-19 with T1D (n = 4).

(F) Quantitative real-time PCR (qPCR) analysis for IFN-γ, TNF-α, and GZMB expression from CD3+Tim-3+T cells in Healthy control (n = 4), COVID-19 (n = 4), patients with T1D (n = 4), and patients with COVID-19 with T1D (n = 4). Horizontal bars represent the mean ± SD. ns, not significant, $^{*}p < 0.05$, $^{**}p < 0.01$, $^{***}p < 0.001$, $^{****}p < 0.0001$ by unpaired Student's t test.

SUPPLEMENTAL INFORMATION

Supplemental information can be found online at https://doi.org/10.1016/j.isci.2025.112339.

Received: July 2, 2024
Revised: November 3, 2024
Accepted: March 31, 2025
Published: April 3, 2025

REFERENCES

1. Sette, A., and Crotty, S. (2021). Adaptive immunity to SARS-CoV-2 and COVID-19. Cell *184*, 861–880.
2. Pezeshki, P.S., and Rezaei, N. (2021). Immune checkpoint inhibition in COVID-19: risks and benefits. Expert Opin. Biol. Ther. *21*, 1173–1179.
3. (2021). The Prevention of Diabetes Mellitus. JAMA *325*, 190.
4. Barnett, R. (2018). Type 1 diabetes. Lancet *391*, 195.
5. Taylor, R. (2013). Type 2 diabetes: etiology and reversibility. Diabetes Care *36*, 1047–1055.
6. Khunti, K., Del Prato, S., Mathieu, C., Kahn, S.E., Gabbay, R.A., and Buse, J.B. (2021). COVID-19, Hyperglycemia, and New-Onset Diabetes. Diabetes Care *44*, 2645–2655.
7. Vlad, A., Serban, V., Timar, R., Sima, A., Botea, V., Albai, O., Timar, B., and Vlad, M. (2021). Increased Incidence of Type 1 Diabetes during the COVID-19 Pandemic in Romanian Children. Medicina *57*, 973.
8. Guo, Y., Bian, J., Chen, A., Wang, F., Posgai, A.L., Schatz, D.A., Shenkman, E.A., and Atkinson, M.A. (2022). Incidence Trends of New-Onset Diabetes in Children and Adolescents Before and During the COVID-19 Pandemic: Findings From Florida. Diabetes *71*, 2702–2706.
9. Accili, D. (2021). Can COVID-19 cause diabetes? Nat. Metab. *3*, 123–125.
10. Codo, A.C., Davanzo, G.G., Monteiro, L.d.B., de Souza, G.F., Muraro, S.P., Virgilio-da-Silva, J.V., Prodonoff, J.S., Carregari, V.C., de Biagi Junior, C.A.O., Crunfli, F., et al. (2020). Elevated Glucose Levels Favor SARS-CoV-2 Infection and Monocyte Response through a HIF-1α/Glycolysis-Dependent Axis. Cell Metab. *32*, 437–446.e5.
11. Wang, J., and Meng, W. (2020). COVID-19 and diabetes: the contributions of hyperglycemia. J. Mol. Cell Biol. *12*, 958–962.
12. Gámez-Díaz, L., and Grimbacher, B. (2021). Immune checkpoint deficiencies and autoimmune lymphoproliferative syndromes. Biomed. J. *44*, 400–411.
13. Liu, L., You, X., Han, S., Sun, Y., Zhang, J., and Zhang, Y. (2021). CD155/TIGIT, a novel immune checkpoint in human cancers (Review). Oncol. Rep. *45*, 835–845.
14. Ara, A., Ahmed, K.A., and Xiang, J. (2018). Multiple effects of CD40-CD40L axis in immunity against infection and cancer. ImmunoTargets Ther. *7*, 55–61.
15. Wolf, Y., Anderson, A.C., and Kuchroo, V.K. (2020). TIM3 comes of age as an inhibitory receptor. Nat. Rev. Immunol. *20*, 173–185.
16. Zahran, A.M., Hetta, H.F., Rayan, A., Eldin, A.S., Hassan, E.A., Fakhry, H., Soliman, A., and El-Badawy, O. (2020). Differential expression of Tim-3, PD-1, and CCR5 on peripheral T and B lymphocytes in hepatitis C virus-related hepatocellular carcinoma and their impact on treatment outcomes. Cancer Immunol. Immunother. *69*, 1253–1263.
17. Huang, S., Liu, D., Sun, J., Zhang, H., Zhang, J., Wang, Q., Gan, L., Qu, G., Qiu, J., Deng, J., et al. (2022). Tim-3 regulates sepsis-induced immunosuppression by inhibiting the NF-κB signaling pathway in CD4 T cells. Mol. Ther. *30*, 1227–1238.
18. Dixon, K.O., Tabaka, M., Schramm, M.A., Xiao, S., Tang, R., Dionne, D., Anderson, A.C., Rozenblatt-Rosen, O., Regev, A., and Kuchroo, V.K. (2021). TIM-3 restrains anti-tumour immunity by regulating inflammasome activation. Nature *595*, 101–106.
19. de Mingo Pulido, Á., Gardner, A., Hiebler, S., Soliman, H., Rugo, H.S., Krummel, M.F., Coussens, L.M., and Ruffell, B. (2018). TIM-3 Regulates CD103(+) Dendritic Cell Function and Response to Chemotherapy in Breast Cancer. Cancer Cell *33*, 60–74.e6.
20. Nakae, S., Iikura, M., Suto, H., Akiba, H., Umetsu, D.T., Dekruyff, R.H., Saito, H., and Galli, S.J. (2007). TIM-1 and TIM-3 enhancement of Th2 cytokine production by mast cells. Blood *110*, 2565–2568.
21. Liu, Y., Chen, Z., Xiao, Y., Chen, H., and Zhou, Z. (2022). Altered expression of Tim family molecules and an imbalanced ratio of Tim-3 to Tim-1 expression in patients with type 1 diabetes. Front. Endocrinol. *13*, 937109.
22. Sánchez-Fueyo, A., Tian, J., Picarella, D., Domenig, C., Zheng, X.X., Sabatos, C.A., Manlongat, N., Bender, O., Kamradt, T., Kuchroo, V.K., et al. (2003). Tim-3 inhibits T helper type 1-mediated auto- and alloimmune responses and promotes immunological tolerance. Nat. Immunol. *4*, 1093–1101.
23. Chen, Z., and John Wherry, E. (2020). T cell responses in patients with COVID-19. Nat. Rev. Immunol. *20*, 529–536.
24. Diao, B., Wang, C., Tan, Y., Chen, X., Liu, Y., Ning, L., Chen, L., Li, M., Liu, Y., Wang, G., et al. (2020). Reduction and Functional Exhaustion of T Cells in Patients With Coronavirus Disease 2019 (COVID-19). Front. Immunol. *11*, 827.
25. Röltgen, K., and Boyd, S.D. (2021). Antibody and B cell responses to SARS-CoV-2 infection and vaccination. Cell Host Microbe *29*, 1063–1075.
26. Yang, H., Xie, T., Li, D., Du, X., Wang, T., Li, C., Song, X., Xu, L., Yi, F., Liang, X., et al. (2019). Tim-3 aggravates podocyte injury in diabetic nephropathy by promoting macrophage activation via the NF-κB/TNF-α pathway. Mol. Metab. *23*, 24–36. https://doi.org/10.1016/j.molmet.2019.02.007.
27. Liu, Y., Pan, Y., Hu, Z., Wu, M., Wang, C., Feng, Z., Mao, C., Tan, Y., Liu, Y., Chen, L., et al. (2020). Thymosin Alpha 1 Reduces the Mortality of Severe Coronavirus Disease 2019 by Restoration of Lymphocytopenia and Reversion of Exhausted T Cells. Clin. Infect. Dis. *71*, 2150–2157.
28. Dixon, K.O., Lahore, G.F., and Kuchroo, V.K. (2024). Beyond T cell exhaustion: TIM-3 regulation of myeloid cells. Sci. Immunol. *9*, eadf2223. https://doi.org/10.1126/sciimmunol.adf2223.
29. Minnie, S.A., Waltner, O.G., Zhang, P., Takahashi, S., Nemychenkov, N.S., Ensbey, K.S., Schmidt, C.R., Legg, S.R.W., Comstock, M., Boiko, J.R., et al. (2024). TIM-3^{+} CD8 T cells with a terminally exhausted phenotype retain functional capacity in hematological malignancies. Sci. Immunol. *9*, eadg1094. https://doi.org/10.1126/sciimmunol.adg1094.
30. Corselli, M., Saksena, S., Nakamoto, M., Lomas, W.E., 3rd, Taylor, I., and Chattopadhyay, P.K. (2022). Single cell multiomic analysis of T cell exhaustion in vitro. Cytometry. A. *101*, 27–44. https://doi.org/10.1002/cyto.a.24496.
31. Ng, C.T., Snell, L.M., Brooks, D.G., and Oldstone, M.B.A. (2013). Networking at the level of host immunity: immune cell interactions during persistent viral infections. Cell Host Microbe *13*, 652–664.
32. Fenwick, C., Joo, V., Jacquier, P., Noto, A., Banga, R., Perreau, M., and Pantaleo, G. (2019). T-cell exhaustion in HIV infection. Immunol. Rev. *292*, 149–163.
33. Avery, L., Filderman, J., Szymczak-Workman, A.L., and Kane, L.P. (2018). Tim-3 co-stimulation promotes short-lived effector T cells, restricts

memory precursors, and is dispensable for T cell exhaustion. Proc. Natl. Acad. Sci. USA *115*, 2455–2460.

34. Nagahara, K., Arikawa, T., Oomizu, S., Kontani, K., Nobumoto, A., Tateno, H., Watanabe, K., Niki, T., Katoh, S., Miyake, M., et al. (2008). Galectin-9 increases Tim-3+ dendritic cells and CD8+ T cells and enhances antitumor immunity via galectin-9-Tim-3 interactions. J. Immunol. *181*, 7660–7669.
35. Qiu, Y., Chen, J., Liao, H., Zhang, Y., Wang, H., Li, S., Luo, Y., Fang, D., Li, G., Zhou, B., et al. (2012). Tim-3-expressing CD4+ and CD8+ T cells in human tuberculosis (TB) exhibit polarized effector memory phenotypes and stronger anti-TB effector functions. PLoS Pathog. *8*, e1002984.
36. Gorman, J.V., Starbeck-Miller, G., Pham, N.L.L., Traver, G.L., Rothman, P.B., Harty, J.T., and Colgan, J.D. (2014). Tim-3 directly enhances CD8 T cell responses to acute Listeria monocytogenes infection. J. Immunol. *192*, 3133–3142.
37. Xue, C., Yao, Q., Gu, X., Shi, Q., Yuan, X., Chu, Q., Bao, Z., Lu, J., and Li, L. (2023). Evolving cognition of the JAK-STAT signaling pathway: autoimmune disorders and cancer. Signal Transduct. Target. Ther. *8*, 204.
38. Villarino, A.V., Gadina, M., O'Shea, J.J., and Kanno, Y. (2020). SnapShot: Jak-STAT Signaling II. Cell *181*, 1696–1696.e1.
39. Hu, X., Li, J., Fu, M., Zhao, X., and Wang, W. (2021). The JAK/STAT signaling pathway: from bench to clinic. Signal Transduct. Target. Ther. *6*, 402.
40. Marroqui, L., Dos Santos, R.S., Fløyel, T., Grieco, F.A., Santin, I., Op de Beeck, A., Marselli, L., Marchetti, P., Pociot, F., and Eizirik, D.L. (2015). TYK2, a Candidate Gene for Type 1 Diabetes, Modulates Apoptosis and the Innate Immune Response in Human Pancreatic β-Cells. Diabetes *64*, 3808–3817.
41. Augustine, G., Sisila, V., Indhu, M., Gupta, D., Tandel, D., Harshan, K.H., Shanmugam, G., Padmapriya, P., Sivasubramanian, S., Kaveri, K., et al. (2023). Redirecting the JAK-STAT signal blocks the SARS-CoV-2 replication. J. Med. Virol. *95*, e28965.
42. Russell, M.A., Richardson, S.J., and Morgan, N.G. (2023). The role of the interferon/JAK-STAT axis in driving islet HLA-I hyperexpression in type 1 diabetes. Front. Endocrinol. *14*, 1270325.
43. Released by National Health Commission & National Administration of Traditional Chinese Medicine (2022). Diagnosis and treatment protocol for COVID-19 patients (Trial Version 9). Health Care Science *1*, 14–28.
44. Alberti, K.G., and Zimmet, P.Z. (1998). Definition, diagnosis and classification of diabetes mellitus and its complications. Part 1: diagnosis and classification of diabetes mellitus provisional report of a WHO consultation. Diabet. Med. *15*, 539–553.

STAR★METHODS

KEY RESOURCES TABLE

REAGENT or RESOURCE	SOURCE	IDENTIFIER
Antibodies		
Anti-CD19-BB700	BD Biosciences	clone SJ25C1; Cat#566396; RRID:AB_2744310
Anti-CD25-APC	BioLegend	clone PC61; Cat#102012; RRID:AB_312861
Anti-CD25-APC	BioLegend	clone M-A2a51; Cat#985810; RRID:AB_2904482
Anti-CD27-PE-CY5	BioLegend	clone M-T271; Cat#356437; RRID:AB_2894486
Anti-CD38-BV510	BioLegend	clone HB-7; Cat#356612; RRID:AB_2563875
Anti-CD39-PE-CY7	BioLegend	clone A1; Cat#328212; RRID:AB_2099950
Anti-CD4-APC/Fire 750	BioLegend	clone SK3; Cat#344637; RRID:AB_2572096
Anti-CD4-AF700	Thermo Fisher Scientific	clone GK1.5; Cat#56-0041-82; RRID:AB_493999
Anti-CD4-BB515	BD Biosciences	clone L200; Cat#564500; RRID:AB_2738828
Anti-CD45RA-eFluor450	Thermo Fisher Scientific	clone HI100; Cat#48-0458-42; RRID:AB_1272059
Anti-CD45RO-BV605	BioLegend	clone UCHL1; Cat#304238; RRID:AB_2562153
Anti-CD69-Percp Cy5.5	BioLegend	clone H1.2F3; Cat#104522; RRID:AB_2260065
Anti-CD69-PE-CY7	Thermo Fisher Scientific	clone FN50; Cat#25-0699-42; RRID:AB_1548714
Anti-CD8-BV650	BioLegend	clone SK1; Cat#344730; RRID:AB_2564510
Anti-CD8a-PE-CY7	BD Biosciences	clone 53-6.7; Cat#552877; RRID:AB_394506
Anti-FOXP3-APC	Thermo Fisher Scientific	clone FJK-16s; Cat#17-5773-82; RRID:AB_469457
Anti-GZMB-PE Dazzle594	BioLegend	clone QA16A02; Cat#372216; RRID:AB_2728383
Anti-GZMB-BV421	BioLegend	clone ICFC; Cat#396413; RRID:AB_2810602
Anti-IFN-γ-AF488	BioLegend	clone XMG1.2; Cat#505813; RRID:AB_493312
Anti-IFN-γ-Percp Cy5.5	BioLegend	clone B27; Cat#506528; RRID:AB_2566187
Anti-Ki-67-BV650	BioLegend	clone 11F6; Cat#151215; RRID:AB_2876504
Anti-Ki-67-Percp-eFlour710	Thermo Fisher Scientific	clone SolA15; Cat#46-5698-82; RRID:AB_11040981
Anti-KLRG1-BV605	BioLegend	clone 2F1/KLRG1; Cat#138419; RRID:AB_2563357
Anti-LAG-3-BV421	BioLegend	clone 11C3C65; Cat#369314; RRID:AB_2629797
Anti-PD-1-APC	BioLegend	clone 29F.1A12; Cat#135209; RRID:AB_2251944
Anti-Tim-3-PE-CY7	BioLegend	clone F38-2E2; Cat#345014; RRID:AB_2561720
Anti-Tim-3-BV785	BioLegend	clone RMT3-23; Cat#119725; RRID:AB_2716066
Anti-Tim-3-PE	BioLegend	clone F38-2E2; Cat#345006; RRID:AB_2116576
Anti-TNF-α-PE	BioLegend	clone MP6-XT22; Cat#506306; RRID:AB_315427
Anti-TNF-α-PE Dazzle594	BioLegend	clone MP6-XT22; Cat#506345; RRID:AB_2565954
TruStain FcX™ PLUS (anti-mouse CD16/32)	BioLegend	clone S17011E; Cat#156604; RRID:AB_2783138
Human TruStain FcX™ (Fc receptor blocking solution)	BioLegend	Cat # 422302; RRID:AB_2818986
Biological samples		
PBMC, serum and plasma from healthy control and COVID-19, T1D, T2D, COVID-19 with T1D patients	N/A	N/A
Chemicals, peptides, and recombinant proteins		
Zombie Aqua™ Fixable Viability Kit	BioLegend	Cat #423101
Standard density gradient centrifugation	Sigma	Cat#10771
TRIzol reagent	Thermo Fisher Scientific	Cat#15596018CN
RevertAid First-Strand cDNA Synthesis Kit	Thermo Fisher Scientific	Cat#K1621
RPIM 1640 medium	Gibco	Cat#31800022

(*Continued on next page*)

Continued

REAGENT or RESOURCE	SOURCE	IDENTIFIER
FBS	CellMax	Cat#SA211.0
CD4 Beads	Beaver	Cat#7090150
CD8 Beads	Miltenyi	Cat#130090859
Deposited data		
RNA-seq datafiles	Mendeley Data	https://doi.org/10.17632/94r6y9jb6g.1 https://doi.org/10.17632/94r6y9jb6g.1 https://doi.org/10.17632/zzf3x4gs24.1 https://doi.org/10.17632/hpmd99x5fn.1 https://doi.org/10.17632/rc63wxj24n.1 https://doi.org/10.17632/vhpkwzgtrm.1 https://doi.org/10.17632/vrvzgf6z69.1 https://doi.org/10.17632/r34jcp2pbr.1
Software and algorithms		
Prism	Graphpad	N/A
FlowJo v 10.7.1	BD Biosciences	N/A
R (version 4.2.2)	www.R-project.org	N/A
Other		
FACS LSRFortessa	BD	N/A
BD FACSymphony S6	BD	N/A
BD FACSymphony A3	BD	N/A
ABI PRISM Step One Sequence Detection System	Applied Biosystems	N/A

EXPERIMENTAL MODEL AND STUDY PARTICIPANT DETAILS

Sample collection

All the patients involved in this study were recruited from the Second Xiangya Hospital. The study included 36 healthy controls, 24 mild-to-moderate COVID-19 patients, 18 severe COVID-19 patients, 10 patients with Type 1 diabetes (T1D), 35 patients with Type 2 diabetes (T2D), 11 COVID-19 patients with T1D, and 52 COVID-19 patients with T2D. Table S1. Participant Demographic Information Table includes information such as the group, gender, age and ethnicity of the participants. Informed consent was provided by all participants, and the study was approved by the Ethics Committee of the Second Xiangya Hospital of Central South University (approval No. SQ2016YFSF110035).

COVID-19 patients were included based on the ‘‘Diagnosis and treatment protocol for COVID-19 patients (Trial Version 9)’’[43] released by the National Health Commission of China and disease severity was classified as follows: (1) Mild-to-moderate COVID-19 is defined as having a blood oxygen saturation level of no less than 93% without the need for oxygen supplementation during hospitalization, with mild clinical symptoms and no or minimal pneumonia manifestations on imaging. (2) Severe COVID-19 is defined as meeting one of the following conditions after excluding other causes: blood oxygen saturation $\leq$93% at rest, ratio of arterial partial pressure of oxygen (PaO2) to fractional inspired oxygen concentration (FiO2) $\leq$300mmHg, respiratory distress with a respiratory rate $\geq$30 breaths per minute, respiratory failure requiring mechanical ventilation, presence of shock; multi-organ dysfunction requiring admission to the intensive care unit (ICU).

Diabetes patients was included based on the diagnostic criteria published by the World Health Organization in 1999,[44] and diabetes types were classified as follows: (1) T1D is defined as dependence on insulin therapy at disease onset, positive test results for at least one classic islet-specific autoantibody (glutamate acid decarboxylase antibody (GADA), zinc transporter 8 antibody (ZnT8A) or insulinoma-associated protein-2 antibody (IA-2A)), or insufficient C-peptide secretion. (2) T2D is defined as insulin resistance and relativity insufficient insulin secretion, negative test results for any pancreatic islet autoantibodies, and no immediate need for insulin treatment.

The inclusion criteria for healthy controls were as follows: Fasting blood glucose levels below 6.1 mmol/L and postprandial blood glucose levels below 7.8 mmol/L.

The exclusion criteria were as follows: patients with other autoimmune diseases, patients with other specific types of diabetes, patients with acute or chronic infections other than COVID-19, patients with recent trauma, surgery, or stress, patients with severe cardiovascular, hepatic, or renal diseases; patients with allergic disorders, patients with malignant tumors, patients with recent occurrence of acute cardiovascular events, patients with mental disorders or infectious diseases; and pregnancy or lactation.

The demographic and clinical data were collected from electronic medical records. All blood samples were collected after obtaining informed consent.

Mice

Age-matched, 8-10-week-old C57BL/6J male and female mice were used for experiments described herein. NOD mice (female, 4–6 weeks old) were purchased from HUAFUKANG Bioscience Co. (Beijing, China). Specific-pathogen-free animal facility at the Experimental Animal Center of Central South University (Changsha, China). All animals had free access to water and food and were group-housed under constant temperature conditions with a 12-h light-dark cycle. Mice were randomly distributed to each experimental group. All animal experiments were conducted in accordance with the guidelines of the Institutional Animal Care and Use Committee of Department of Laboratory Animal Science, Central South University (approval No. 20230650).

Peripheral blood mononuclear cells (PBMCs) and T cells isolation

Fresh human venous blood samples were collected on an empty stomach into EDTA test tubes and processed within 2 h. Peripheral blood mononuclear cells (PBMCs) were separated using standard density gradient centrifugation (Cat#10771, Sigma). Mouse spleen cells were obtained as a single cell suspension, and purified CD4+T cells and CD8+T cells were obtained through negative selection with CD4 (Cat#7090150, Beaver) or CD8 (Cat#130090859, Miltenyi) magnetic beads. Human CD3+Tim-3+ T cells and CD3+Tim-3- T cells were sorted by flow cytometry from patients with HC, COVID-19, T1D, and COVID-19 with T1D.

METHOD DETAILS

Isolation of RNA

TRIzol reagent (Invitrogen, Thermo Fisher Scientific, Cat#15596018CN) was used to harvest total RNA from the CD3+T cells, and the RNA concentration was quantified by measuring the ultraviolet absorbance at 260 nm. Equal amounts of RNA (1μg) were converted to complementary deoxyribonucleic acid (cDNA) with a RevertAid First-Strand cDNA Synthesis Kit (Thermo Fisher Scientific, Cat#K1621) according to the manufacturer's instructions.

The cytokine secretion capability and phenotype of T cell

Freshly isolated mouse spleen cells were plated in a 48-multiwell plate at the concentration of 0.5 × 105 cells/well in 500ul of complete culture medium, composed of RPIM 1640 medium (Gibco) supplemented with 10% FBS (CellMax), 1% Penicillin–Streptomycin and 1% L-glutamine. The plate was pre-coated anti-CD3 antibody (2ug/ml) and incubated 2 h before cell plating. Cells were then cultured in the presence of anti-CD28 (5ug/ml) antibody and IL-2 (10 ng/ml) for 3 days. Cell stimulation cocktail (1μL/well) was added to stimulate the cells. After 4–6 h of stimulation, cells were collected for flow cytometry analysis.

Flow cytometry

To detect the frequency of various T cell subsets and their Tim-3 expression levels, PBMCs were stained on the surface and intracellularly with anti-human or anti-mouse mAbs. For surface staining, cells were incubated with Zombie Aqua Fixable Viability Kit (BioLegend) in PBS for 10 min at 4°C to distinguish viable and dead cells. For non-specific binding blocking, cell were stained with FcR reagent for mice (BioLegend Cat# 156604, RRID: AB_2783138) and human (BioLegend Cat# 422302, RRID:AB_2818986) for 10 min at 4°C respectively. Cells were stained with surface fluorescently labeled monoclonal antibodies in D-hanks buffer (Cat#H1040, Solarbio) supplemented with 0.5% BSA for 30 min at 4°C. For intracellular staining, after staining for surface antigens, cells were permeablized with Fixation & Permeabilization Buffer (Cat#00552300, eBioscience). The monoclonal antibodies are as follows: APC/Fire 750 anti-human CD4 (BioLegend Cat# 344637, RRID:AB_2572096), BV650 anti-human CD8 (BioLegend Cat# 344730, RRID:AB_2564510), eFluor450 anti-human CD45RA (Thermo Fisher Scientific Cat# 48-0458-42, RRID:AB_1272059), BV605 anti-human CD45RO (BioLegend Cat# 304238, RRID:AB_2562153), BB700 anti-human CD19 (BD Biosciences Cat# 566396, RRID:AB_2744310), PE-CY5 anti-human CD27(BioLegend Cat# 356437, RRID:AB_2894486), BV510 anti-human CD38(BioLegend Cat# 356612, RRID:AB_2563875), PE-CY7 anti-human CD366(Tim-3) (BioLegend Cat# 345014, RRID:AB_2561720). AF700 anti-mouse CD4 (Thermo Fisher Scientific Cat# 56-0041-82, RRID:AB_493999), PE-CY7 anti-mouse CD8a(BD Biosciences Cat# 552877, RRID:AB_394506), AF488 anti-mouse IFN-γ(BioLegend,Cat#505813), APC anti-mouse FOXP3(Thermo Fisher Scientific Cat# 17-5773-82, RRID:AB_469457), PE Dazzle594 anti-mouse GZMB(BioLegend Cat# 372216, RRID:AB_2728383), Percp Cy5.5 anti-mouse CD69(BioLegend Cat# 104522, RRID:AB_2260065), APC anti-mouse CD25(BioLegend Cat# 102012, RRID:AB_312861), PE anti-mouse TNF-α(BioLegend Cat# 506306, RRID:AB_315427), BV785 anti-mouse Tim-3(BioLegend Cat# 119725, RRID:AB_2716066), BV650 anti-mouse Ki-67(BioLegend Cat# 151215, RRID:AB_2876504). The flow cytometry antibodies mentioned above were diluted and applied according to the optimal concentration specified in the instruction manual. The detailed information about the antibodies is provided in the Supplementary table.

RNA-seq

Mouse spleen cells were obtained as a single cell suspension, and purified CD4+T cells and CD8+T cells were obtained through negative selection with CD4 (Cat#7090150, Beaver) or CD8 (Cat#130090859, Miltenyi) magnetic beads. The cells were plated onto anti-CD3 (2ug/ml) -coated 48-well plates, supplemented with and anti-CD28 (5ug/ml) and IL-2 (10ug/ml). After 3 days, these cells were collected, stained with Zombie Aqua Fixable Viability Kit (BioLegend) and BV785 anti-mouse Tim-3 (BioLegend Cat# 119725, RRID: AB_2716066), and then sorted into Tim-3+CD4+T cells, Tim-3-CD4+T cells, Tim-3+CD8+T cells, Tim-3-CD8+T

cells through the flow sorting technology. After washing twice with PBS, 1mL Trizol was added to extract RNA and send for inspection.

Quantitative real-time PCR

After PBMC preparation, the single cell suspension from human was purified to obtain CD3+Tim-3+T cells and CD3+Tim-3-T cells through fluorescence-activated cell sorting (BD FAC SymphonyTmS6). After RNA isolation, the synthesized cDNAs were amplified with oligonucleotides specific for JAK1, STAT1, and STAT2, which were key molecules in the signaling pathway significantly associated with Tim-3 expression in the RNA-seq result. Quantitative real-time PCR was performed on an ABI PRISM Step One Sequence Detection System (Applied Biosystems, Carlsbad, CA, USA).

The primers were used as follows: human-β-actin (F: CATGTACGTTGCTATCCAGGC, R: CTCCTTAATGTCACGCACGAT), human-JAK1(F: CTTTGCCCTGTATGACGAGAAC, R: ACCTCATCCGGTAGTGGAGC), human-STAT1(F: CAGCTTGACTCAAAATTCCTGGA, R: TGAAGATTACGCTTGCTTTTCCT), human-STAT2(F: CCAGCTTTACTCGCACAGC, R: AGCCTTGGAATCATCACTCCC).

QUANTIFICATION AND STATISTICAL ANALYSIS

Statistical analyses were performed using GraphPad Prism 9 software and R 4.2.2. Data were presented as the mean ± standard deviation (SD) of at least three independent experiments, or as the median (25th, 75th percentiles) for abnormally distributed data. One-way ANOVA models were utilized to compare three or more independent groups. Paired t-test was employed to compare the functional changes of Tim-3+ and Tim-3- in the same sample. Associations between the frequencies of all T cell subset and clinical indicators of disease progression were evaluated with Spearman's correlation. A p-value of 0.05 or less was considered statistically significant.